Penicillin-binding protein folding is dependent on the PrsA peptidyl-prolyl cis-trans isomerase in Bacillus subtilis

Hyyrylainen, Hanne-Leena; Marciniak, Bogumila C.; Dahncke, Kathleen; Pietiainen, Milla; Courtin, Pascal; Vitikainen, Marika; Seppala, Raili; Otto, Andreas; Becher, Doerte; Chapot-Chartier, Marie-Pierre

Published in:
Molecular Microbiology

DOI:
10.1111/j.1365-2958.2010.07188.x

Publication date:
2010

Molecular Microbiology (2010) 77(1), 108–127 ■
doi:10.1111/j.1365-2958.2010.07188.x
First published online 13 May 2010

Penicillin-binding protein folding is dependent on the PrsA peptidyl-prolyl *cis-trans* isomerase in *Bacillus subtilis*

Hanne-Leena Hyyryläinen,[1] Bogumila C. Marciniak,[2] Kathleen Dahncke,[3†] Milla Pietiäinen,[1] Pascal Courtin,[4] Marika Vitikainen,[1‡] Raili Seppala,[1] Andreas Otto,[3] Dörte Becher,[3] Marie-Pierre Chapot-Chartier,[4] Oscar P. Kuipers[2] and Vesa P. Kontinen[1]*

[1]*Antimicrobial Resistance Unit, Department of Infectious Disease Surveillance and Control, National Institute for Health and Welfare (THL), P.O. Box 30, FI-00271 Helsinki, Finland.*
[2]*Molecular Genetics Group, Groningen Biomolecular Sciences and Biotechnology Institute, University of Groningen, Kerklaan 30, 9751 NN Haren, the Netherlands.*
[3]*Institut für Mikrobiologie, Ernst-Moritz-Arndt Universität Greifswald, Friedrich-Ludwig-Jahn-Str. 15, D-17489 Greifswald, Germany.*
[4]*INRA, UR477 Biochimie Bactérienne, F-78350 Jouy-en-Josas, France.*

Summary

The PrsA protein is a membrane-anchored peptidyl-prolyl *cis-trans* isomerase in *Bacillus subtilis* and most other Gram-positive bacteria. It catalyses the post-translocational folding of exported proteins and is essential for normal growth of *B. subtilis*. We studied the mechanism behind this indispensability. We could construct a viable *prsA* null mutant in the presence of a high concentration of magnesium. Various changes in cell morphology in the absence of PrsA suggested that PrsA is involved in the biosynthesis of the cylindrical lateral wall. Consistently, four penicillin-binding proteins (PBP2a, PBP2b, PBP3 and PBP4) were unstable in the absence of PrsA, while muropeptide analysis revealed a 2% decrease in the peptidoglycan cross-linkage index. Misfolded PBP2a was detected in PrsA-depleted cells, indicating that PrsA is required for the folding of this PBP either directly or indirectly. Furthermore, strongly increased uniform staining of cell wall with a fluorescent vancomycin was observed in the absence of PrsA. We also demonstrated that PrsA is a dimeric or oligomeric protein which is localized at distinct spots organized in a helical pattern along the cell membrane. These results suggest that PrsA is essential for normal growth most probably as PBP folding is dependent on this PPIase.

Accepted 19 April, 2010. *For correspondence. E-mail vesa.kontinen@thl.fi; vesa.p.kontinen@helsinki.fi; Tel. (+358) 20 610 68562; Fax (+358) 20 610 68238. Present addresses: †Abteilung Biochemie der Pflanzen, Institut für Biologie, Freie Universität Berlin, Königin-Luise-Straße 12-16, D-14195 Berlin, Germany; ‡VTT Technical Research Centre of Finland, Biotechnology, Tietotie 2, Espoo, P.O. Box 1000, FI-02044 VTT, Finland.

Introduction

Intracellular folding of a protein into a native functional structure is assisted by molecular chaperones and foldase enzymes. A class of foldases ubiquitous in all types of cells and cell compartments is formed by peptidyl-prolyl *cis-trans* isomerases (PPIases), which catalyse the isomerization of peptide bonds immediately preceding proline residues (Schiene and Fischer, 2000; Wang and Heitman, 2005; Lu and Zhou, 2007). Three families of PPIases have been identified: cyclophilins, FK506-binding proteins and parvulins (Rahfeld *et al.*, 1994). The archetype of the parvulin family of PPIases is the *Escherichia coli* Par10, which consists of 92 amino acid residues comprising the minimal catalytic domain (Kühlewein *et al.*, 2004). In other parvulins, a catalytic domain is flanked with N- and C-terminal regions of various lengths and roles in substrate binding and/or chaperone-like catalysis of folding (Lu *et al.*, 1996; Yaffe *et al.*, 1997; Uchida *et al.*, 1999; Wu *et al.*, 2000; Behrens *et al.*, 2001; Vitikainen *et al.*, 2004). Human Pin1 and its counterpart parvulins in other eukaryotic cells specifically recognize proline residues that are preceded by phosphorylated serine or threonine residues (Hani *et al.*, 1999; Lu *et al.*, 1999; Yao *et al.*, 2001; Lu and Zhou, 2007). Other parvulins have a wider substrate range, as their substrate recognition is independent of phosphorylation (Hennecke *et al.*, 2005; Stymest and Klappa, 2008).

PrsA is a lipoprotein bound to the outer face of the cytoplasmic membrane in *Bacillus subtilis* and other Gram-positive Firmicutes (Kontinen and Sarvas, 1993; Vitikainen *et al.*, 2004). It consists of a diacylglycerol membrane anchor, a large functionally unknown N-terminal domain followed by a PPIase domain with similarity to the parvulin

family of PPIases and a small functionally unknown C-terminal domain (Vitikainen *et al*., 2004). *Bacillus subtilis* PrsA exhibits PPIase activity but may also have a chaperone-like activity *in vivo* (Vitikainen *et al*., 2004). The presence of a deletion in the PPIase domain of the *Lactococcus lactis* PrsA-like protein PmpA suggests that it may function only as a chaperone (Drouault *et al*., 2002). The periplasmic SurA of *E. coli* is also a chaperone with a specialized role in the folding and assembly of outer-membrane proteins (Behrens *et al*., 2001). Several extracellular proteins in various Gram-positive bacteria are secreted or maturated in a PrsA-dependent manner (Kontinen and Sarvas, 1993; Hyyryläinen *et al*., 2000; Vitikainen *et al*., 2001, 2005; Drouault *et al*., 2002; Lindholm *et al*., 2006; Ma *et al*., 2006; Alonzo *et al*., 2009; Zemansky *et al*., 2009). Overexpression of PrsA enhances α-amylase secretion from *Bacillus* and *L. lactis* cells (Kontinen and Sarvas, 1993; Vitikainen *et al*., 2001, 2005; Lindholm *et al*., 2006) including the biotechnically important thermoresistant AmyL α-amylase of *Bacillus licheniformis* (Kontinen and Sarvas, 1993). Some other extracellular proteins are also secreted at increased levels from PrsA-overexpressing cells (Wu *et al*., 1998; Williams *et al*., 2003). In *B. subtilis*, PrsA is an essential cell component in normal growth conditions indicating that it has an indispensable role in protein folding at the membrane-cell wall interface ('periplasm') (Vitikainen *et al*., 2001). All three domains are essential for PrsA function (Vitikainen *et al*., 2004). Inactivation of the D-alanylation system of the teichoic acids (Dlt) restores slight growth of *B. subtilis* cells lacking PrsA, suggesting that the increased net negative charge of the wall in the absence of Dlt partially suppresses the growth defect (Hyyryläinen *et al*., 2000). In contrast to the rod-shaped *B. subtilis*, PrsA is a dispensable protein in several cocci, *L. lactis* (Drouault *et al*., 2002), *Streptococcus pyogenes* (Ma *et al*., 2006) and *Staphylococcus aureus* (Vitikainen *et al*., unpublished).

In this study our purpose was to identify the indispensable cell component(s) which is (are) folded in a PrsA-dependent manner and to elucidate why PrsA is an essential protein in the rod-shaped bacterium *B. subtilis,* but non-essential in cocci. A hypothesis explaining this difference could be that PrsA catalyses the folding of a protein(s) involved in the biosynthesis of the cylindrical (lateral) cell wall and determination of the rod cell shape. The bacterial cell shape is maintained by a peptidoglycan cell wall (murein sacculus) and the actin-like proteins Mbl, MreB and MreBH, which form helical cables (cytoskeleton) that encircle the cell immediately beneath the cell membrane (Jones *et al*., 2001; Carballido-Lopez and Errington, 2003; Soufo and Graumann, 2003; Defeu Soufo and Graumann, 2004; Stewart, 2005; Kawai *et al*., 2009). The rod shape of *B. subtilis* is also dependent on other proteins including MreC and MreD, which are membrane proteins and interact with each other and Mbl (Defeu Soufo and Graumann, 2006; van den Ent *et al*., 2006). In the absence of any of these Mre proteins, cells are spherical or aberrant in shape or non-viable in normal growth conditions (Jones *et al*., 2001; Leaver and Errington, 2005; Kawai *et al*., 2009). Studies on the cell shape determination of *Caulobacter crescentus* and *B. subtilis* have also shown that MreB, MreC and MreD interact with penicillin-binding proteins (PBPs) (Figge *et al*., 2004; Divakaruni *et al*., 2005; van den Ent *et al*., 2006; Kawai *et al*., 2009). Peptidoglycan precursors are incorporated into the wall at distinct sites organized in a helical pattern along the lateral wall (Daniel and Errington, 2003; Tiyanont *et al*., 2006; Divakaruni *et al*., 2007). The Mre proteins and two PBP1-associated cell division proteins, EzrA and GpsB, are involved in the determination of the spatial organization and dynamics of the peptidoglycan synthesis (Claessen *et al*., 2008; Kawai *et al*., 2009). In *Corynebacterium glutamicum*, which does not have the *mreB* gene (Daniel and Errington, 2003), peptidoglycan precursors are incorporated for the whole lateral wall via the newly formed division poles. In *S. aureus* and probably in cocci more generally, peptidoglycan synthesis takes place only at the division septum and the hemispherical poles derived from it after cell division (Pinho and Errington, 2003).

High-molecular-weight PBPs are membrane-bound transglycosylase and transpeptidase enzymes which use peptidoglycan precursors to synthesize peptidoglycan chains and cross-link adjacent glycan chains to form a murein sacculus (Popham and Young, 2003; Sauvage *et al*., 2008). Class A high-molecular-weight PBPs possess both transglycosylase and transpeptidase activities, whereas class B high-molecular-weight PBPs have only transpeptidase activity (Scheffers *et al*., 2004). In addition to these two classes of high-molecular-weight PBPs, bacterial cells also contain low-molecular-weight PBPs (class C) which have neither transglycosylase nor transpeptidase activity, but function as carboxypeptidases or endopeptidases (Popham and Young, 2003; Sauvage *et al*., 2008). The *B. subtilis* genome sequence has revealed 16 PBP-encoding genes, many of which are functionally redundant (Scheffers *et al*., 2004). The PBPs have several distinct localization patterns in the cell suggesting dedicated functional roles for them in cell wall growth or cell division (Scheffers *et al*., 2004). The PBP3 and PBP4a monofunctional transpeptidases and the PBP5 D-alanyl-D-alanine carboxypeptidase are localized in distinct spots or bands in the region of the lateral cell wall, suggesting their involvement in the elongation of the lateral wall. The bifunctional PBP1 is involved in the growth of both the lateral wall and the septum (Pedersen *et al*., 1999; Scheffers *et al*., 2004; Claessen *et al*., 2008; Kawai *et al*., 2009). The PBP2a and PbpH transpeptidases have a redundant, essential activity in the lateral wall synthesis and rod-shape determination

(Wei *et al.*, 2003), whereas the septal localization of PBP2b suggests a specific role for this transpeptidase in cell division (Scheffers *et al.*, 2004).

MreC and PBPs possess a number of proline residues (about 3% of amino acid residues) and the functional domains of these proteins are localized in the same cell compartment as PrsA suggesting that their folding could be dependent on PrsA. Misfolded proteins are rapidly degraded by the quality-control proteases such as HtrA (Hyyryläinen *et al.*, 2001). We studied the stability of MreC and PBPs in cells depleted of PrsA to find out whether misfolding of these proteins occurs in the absence of PrsA. Stabilities of three divisome proteins with a 'periplasmic' domain, FtsL, DivIB and DivIC (Daniel *et al.*, 1998; Katis and Wake, 1999) were also determined in a similar manner. Membrane proteomes were analysed to identify other possible PrsA-dependent membrane proteins. Various methods and approaches including electron microscopy, muropeptide analysis and labeling of PBPs and peptidoglycan precursors with fluorescent antibiotics were used to characterize the cell wall biosynthesis defect of PrsA-depleted cells and the functional role of PrsA in cell shape determination. Furthermore, we studied whether PrsA is evenly or non-evenly distributed along the cell membrane. The results showed that several PBPs are folded in a PrsA-dependent manner, suggesting that this is the likely cause for the growth arrest in the absence of PrsA.

Results

B. subtilis *cells depleted of the PrsA protein are able to grow in the presence of a high concentration of magnesium*

In order to modulate cellular amount of PrsA, we have placed the *B. subtilis prsA* gene under the transcriptional control of the IPTG-inducible P*spac* promoter (Vitikainen *et al.*, 2001). Transmission electron microscope images of cells expressing P*spac-prsA* (IH7211) at low levels showed that PrsA depletion causes distinct changes in cell morphology. Severely PrsA-depleted cells which were still able to grow (P*spac-prsA* induced with 8 μM IPTG) were rod shaped but much larger than cells of the parental wild-type strain (compare Fig. 1A and B). At a PrsA level that was insufficient to support normal growth, large spherical cells were observed (Fig. 1C and D). Thick cell wall material was seen in residual division septa between the spherical cells, whereas in the periphery in many sites only a thin wall layer was left, suggesting that PrsA may be required for the biosynthesis of the lateral cell wall. These changes in cell morphology are similar to those seen in defects of the cell wall polymer biosynthesis and cell shape determination (Wei *et al.*, 2003; Leaver and Errington, 2005).

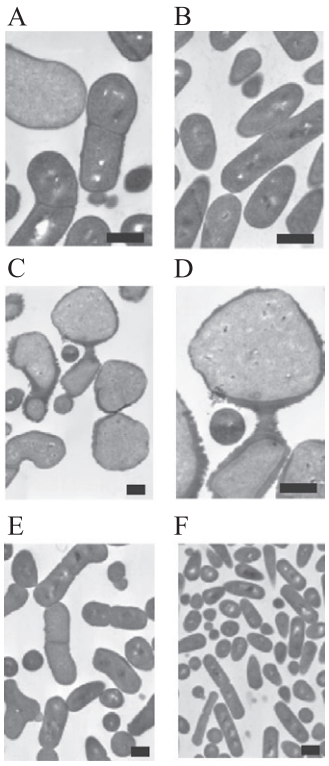

Fig. 1. Morphological changes of PrsA-depleted cells. Electron microscopy of PrsA-depleted cells was performed as described in *Experimental procedures*. The scale bars – 2 μm.
A. IH7211 (P*spac-prsA*) induced with 8 μM IPTG.
B. RH2111 wild-type strain.
C–D. IH7211 (P*spac-prsA*) in the absence of IPTG.
E. IH7211 (P*spac-prsA*) in the absence of IPTG and in the presence of 20 mM $MgCl_2$.
F. IH7211 (P*spac-prsA*) induced with 1 mM IPTG.

The MreC and MreD cell shape-determination proteins are required for lateral cell wall biosynthesis and normal growth of *B. subtilis*. However, a high concentration of magnesium (20 mM) in the growth medium restores some growth even in the complete absence of these proteins (Leaver and Errington, 2005). Cells depleted of MreC or MreD in the presence of 20 mM magnesium are spherical in shape. The mechanism of this suppression is currently unknown. Because magnesium also rescues growth of other mutants with defects in different aspects of cell wall biosynthesis (Δ*ponA* and Δ*mreB*), and which in contrast to *mreC* and *mreD* mutants maintain a wild type-like rod shape, it may affect indirectly peptidoglycan structure or turnover (Formstone and Errington, 2005). We studied whether the growth defect of PrsA-depleted cells can be suppressed by magnesium. The strain IH7211 (P*spac-prsA*) was grown in Antibiotic Medium 3 in the presence or absence of IPTG and the effect of 20 mM $MgCl_2$ on the growth was determined. Interestingly, magnesium restored the growth of PrsA-depleted IH7211 (Fig. 2). However, even though the PrsA-depleted cells grew in the

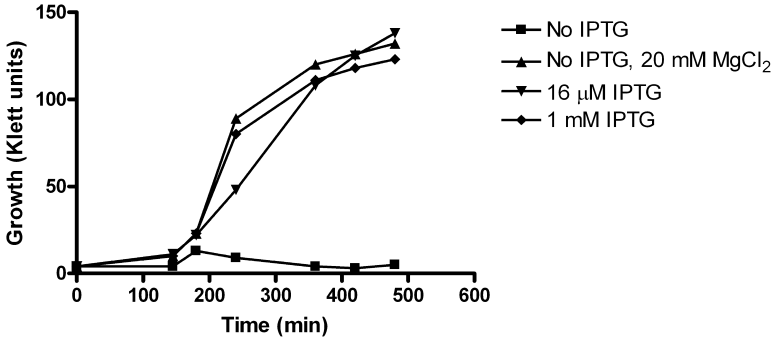

Fig. 2. The suppression of the growth defect of PrsA-depleted cells by 20 mM $MgCl_2$. Cells of IH7211 (P*spac-prsA*) were grown in Antibiotic Medium 3 with the supplementations indicated.

presence of magnesium, it did not restore the 'normal' morphology of PrsA-expressing cells but they remained thick rods (Fig. 1E and F).

PrsA is required for the stability of several penicillin-binding proteins

The above results suggest that PrsA is involved in the folding of a membrane protein(s) which has (have) a large 'periplasmic' domain with an essential role(s) in the wall biosynthesis and/or cell shape determination. We used N-terminal green fluorescence protein (GFP) tags and specific antibodies against GFP, MreC and PrsA to determine effects of the PrsA depletion on the stability of potential PrsA-dependent membrane components. We started this study with GFP fusions, as most of these constructs were available and used previously in other studies (Scheffers *et al*., 2004; Leaver and Errington, 2005). We were particularly interested in finding out whether the stability of MreC and PBPs is dependent on PrsA. The PBP 2b (PBP2b) interacts with the divisome proteins DivIB, DivIC and FtsL and affects their stability (Daniel *et al*., 2006). Furthermore, an NMR study of DivIB suggested that *cis-trans* isomerization of a specific prolyl peptide bond causes a major structural change in this divisome protein and it was proposed that the *cis-trans* isomerization may function as a regulatory switch in cell division (Robson and King, 2006). Therefore, we were also interested in determining the stability of DivIB, DivIC and FtsL in PrsA-depleted cells.

The absence of PrsA did not decrease cellular levels of MreC and GFP-MreC as determined by immunoblotting with anti-MreC antibodies, suggesting that PrsA is not essential for the folding and stability of this cell shape-determination protein (Fig. S1). Hence, despite of the similar suppression of the growth defects of PrsA-depleted and MreC-depleted cells by magnesium, the growth inhibition in the absence of PrsA is most probably not caused by misfolding of MreC. In contrast, PBP2a, a high-molecular-weight PBP, which is involved in the lateral cell wall biosynthesis (Wei *et al*., 2003), is most probably a PrsA-dependent protein, as indicated by a clear decrease in the level of GFP-PBP2a in PrsA-depleted cells expressing this fusion protein (Fig. 3A) and in their isolated membranes (Fig. S1). The PrsA dependency of PBP1a/b, the largest of the PBPs of *B. subtilis*, was also studied with a GFP-PBP1a/b construct. GFP-PBP1a/b was stable in PrsA-depleted cells (Fig. S1), suggesting that PBP1a/b folding is independent of PrsA. The PrsA-dependency analysis of the DivIB, DivIC and FtsL divisome proteins revealed that none of them are PrsA dependent (Fig. S2).

The binding of β-lactam antibiotics to the native fold of PBPs can be used to visualize and determine cellular levels of enzymatically active PBPs. In order to elucidate the effect of the PrsA depletion on the levels of correctly folded PBPs, cell membranes were isolated from PrsA-depleted and non-depleted cells and PBPs were labeled with fluorescent penicillin, Bocillin-FL, and analysed with SDS-PAGE. There are 16 PBPs in *B. subtilis* and seven of them, PBP1a/b, PBP2a, PBP2b, PBP2c, PBP3, PBP4 and PBP5, could be identified with Bocillin-FL labeling (Fig. 3B). The identification of these PBPs is based on a similar labeling experiment with null mutants of the corresponding genes with the exception of PBP2b (Fig. S3) and their known migration in SDS-PAGE as determined in a previous study by another group (Popham and Setlow, 1996). The level of PBP2c encoded by the *pbpF* gene was clearly lower than the levels of the other PBPs. It was detected as a very weak band below the band of PBP2b (Fig. 3B and Fig. S3). The two forms of PBP1, a and b (Popham and Setlow, 1995), could not be separated in the mini-gels used in this analysis. The data demonstrate that four out of seven PBPs were affected by the PrsA depletion (Fig. 3B). The levels of active PBP2a, PBP2b, PBP3 and PBP4 were clearly lower in cells 'lacking' PrsA as compared with non-depleted cells, suggesting that their stability is dependent on the PrsA foldase, whereas the levels of PBP1a/b, PBP2c and PBP5 were not decreased, suggesting their independence of PrsA. These results are consistent with the similar effects of the PrsA depletion on GFP-PBP2a and GFP-PBP1a/b observed in the above immunoblotting experiments. The levels of the four PrsA-dependent PBPs were decreased in a similar manner also

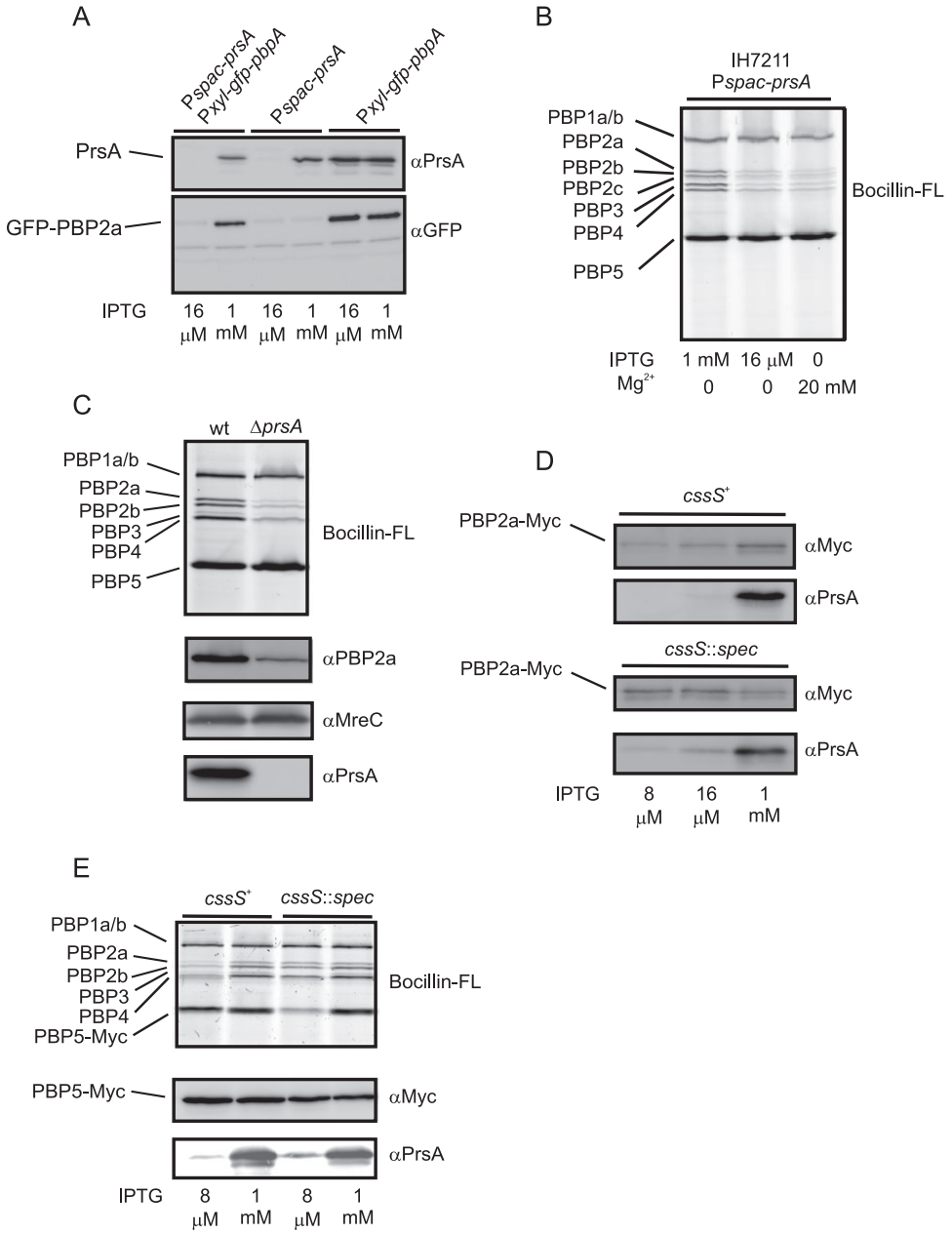

Fig. 3. PrsA depletion destabilizes penicillin-binding proteins.
A. Effect of PrsA depletion on the cellular level of GFP-PBP2a. Whole cell samples from *B. subtilis* IH8437 (P*xyl-gfp-pbpA* P*spac-prsA*) were prepared as described in *Experimental procedures* and levels of GFP-PBP2a and PrsA were determined by immunoblotting and chemiluminescence detection. P*xyl* was induced with 0.5% xylose.
B. Cytoplasmic membranes were isolated and levels of active PBPs were visualized by staining with Bocillin-FL (see *Experimental procedures*) and separation in SDS-PAGE. Effect of PrsA depletion and magnesium on the levels of active PBPs. The genes encoding PBP1a/b, PBP2a, PBP2b, PBP2c, PBP3, PBP4 and PBP5 are *ponA*, *pbpA*, *pbpB*, *pbpF*, *pbpC*, *pbpD* and *dacA* respectively.
C. Effect of the *prsA* null mutation (Δ*prsA*; *B. subtilis* IH9024) on levels of active PBPs (Bocillin FL staining) and total levels of PBP2a, MreC and PrsA (immunoblotting).
D. Levels of PBP2a-Myc in PrsA-depleted cells in the presence (*B. subtilis* IH9027; *pbpA-myc* P*spac-prsA*) and absence of CssS (*B. subtilis* IH9016; *pbpA-myc* P*spac-prsA cssS*::*spec*) as determined by immunoblotting.
E. Misfolding of PBP5-Myc in the absence of both PrsA and CssS. Bocillin-FL staining of active PBPs and immunoblotting of total PBP5-Myc in membranes of PrsA-depleted and non-depleted cells of IH9028 (*dacA-myc* P*spac-prsA*) and IH9029 (*dacA-myc* P*spac-prsA cssS*::*spec*).

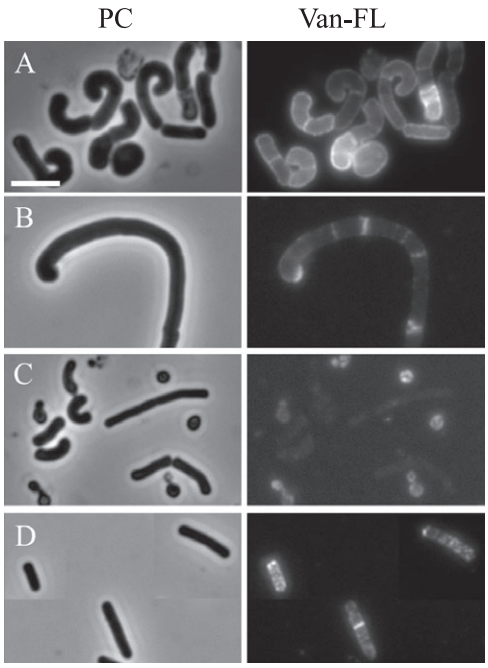

Fig. 4. Van-FL staining of *B. subtilis* Δ*prsA* mutant IH9024 (A–C) and 168 (D). Left panels – phase contrast images, right panels – Van-FL staining. Scale bar represents 6 μm (the same for all the images).
A. and D. Exponential growth phase.
B. Stationary phase.
C. Late stationary phase.

in the presence of 20 mM $MgCl_2$, suggesting that magnesium does not suppress their instability (Fig. 3B).

The prsA *gene can be deleted in the presence of a high concentration of magnesium*

The suppression of the growth defect of PrsA-depleted *B. subtilis* IH7211 cells in the presence of a high concentration of magnesium suggests that it might be possible to construct a *prsA* null mutant (gene replacement) on plates supplemented with magnesium. Indeed this was the case (see *Experimental procedures* for the mutant construction). The *prsA* null mutant grew on Antibiotic Medium 3 – plates supplemented with 20 mM $MgCl_2$ forming very tiny homogeneous colonies. Microscopic inspection of cells in the colonies showed that all bacteria were strongly deformed: either giant vesicular cells or thick twisted rods. These cells looked quite similar as PrsA-depleted cells of IH7211. In corresponding liquid cultures, the large deformed cells changed so that in overnight grown cultures small motile cocci-like cells, short bent rods, which were thinner than those in the exponential growth phase, and also fairly normal-looking rods were observed (see Fig. 4). The appearance of viable cocci-like *prsA* null mutant cells corroborates the evidence about the involvement of PrsA in lateral cell wall biosynthesis and cell elongation. However, the presence of some rod-shaped bacteria in overnight cultures suggests that they were capable of synthesizing the cylindrical lateral wall in the absence of PrsA. We did not see on plates any fast-growing suppressors that would have overgrown the more slowly growing Δ*prsA* mutant.

Bocillin-FL labeling of *prsA* null mutant membranes showed that the level of activity of the same set of PBPs as in the case of PrsA-depleted IH7211 (PBP2a, PBP2b, PBP3 and PBP4) was decreased (Fig. 3C). Again, no effect was seen on PBP1a/b and PBP5. There was some experimental variation in the staining of PBP3 in membranes from PrsA-expressing strains (compare Fig. 3B and C), but not with the other PBPs. It may be more unstable than the other ones. We also determined protein levels of PBP2a and MreC in the null mutant and the wild-type parental strain by immunoblotting with anti-PBP2a and anti-MreC antibodies respectively. The PBP2a amount was clearly lower (> 50% reduction) in the absence of PrsA (Fig. 3C), whereas like in the case of PrsA-depleted IH7211 no effect of PrsA was seen on the MreC amount. This result suggests that in the absence of PrsA significant misfolding and degradation of several PBPs occurs. PrsA may not be involved in the folding of MreC.

The CssRS two-component system is involved in the quality control of penicillin-binding proteins

There are several 'periplasmic' proteases which could be involved in the quality control and degradation of PBPs including HtrA, HtrB, PrsW and WprA (Margot and Karamata, 1996; Stephenson and Harwood, 1998; Hyyryläinen *et al*., 2001; Ellermeier and Losick, 2006; Heinrich *et al*., 2008). Accumulation of misfolded proteins in the cell wall (misfolding or secretion stress) induces *htrA* and *htrB* gene expression in a manner dependent on the CssRS two-component system (Hyyryläinen *et al*., 2001; Darmon *et al*., 2002). CssRS is most probably dedicated to regulate the expression of only these two quality control protease genes (Hyyrylainen *et al*., 2005). We used a knockout mutation of the *cssS* gene (*cssS::spec*) to study whether CssRS and the HtrA/B proteases it specifically regulates are involved in PBP degradation. We constructed strains which express PBP2a-Myc or PBP5-Myc proteins (PBPs modified with a C-terminal Myc-tag) and determined their levels in the presence and absence of *cssS::spec* and in PrsA-depleted and non-depleted cells by immunoblotting with anti-Myc antibodies. Bocillin-FL staining was also used to determine levels of active correctly folded PBPs in the *cssS::spec* mutant cells.

Immunoblotting revealed that the *cssS::spec* mutation decreased PBP2a-Myc degradation in PrsA-depleted cells (Fig. 3D), suggesting that HtrA and HtrB proteases are

involved in the degradation of misfolded PBP2a. The amount of PBP5-Myc as determined by immunoblotting was not significantly affected by *cssS::spec* (Fig. 3E). It was independent of CssRS and PrsA. However, Bocillin-FL labeling revealed that in the absence of CssS the level of active PBP5-Myc was clearly lower in PrsA-depleted cells than in non-depleted cells (Fig. 3E). The PrsA depletion and *cssS::spec* mutation alone had no effect on the level of active PBP5-Myc. These results show that CssRS, probably via HtrA/B proteases, and PrsA both are involved in the formation (folding) of active PBP5 (an overlapping function). The Bocillin-FL labeling (Fig. 3E) also suggested that absence of CssS (and HtrA/B proteases) increased the level of active PBP2a, PBP2b and PBP4 in PrsA-depleted cells. It seems that if PBP2a degradation is prevented (*cssS::spec*), at least some active correctly folded PBP2a is nevertheless formed with time despite of the absence or very low level of PrsA. PBP2a and PBP5 are quite different in this respect.

Incorrectly folded PBP2a is formed in PrsA-depleted cells

In order to demonstrate that PrsA-depletion causes misfolding of PBP2a, we quantitated the levels of PBP2a-Myc in membranes of PrsA-depleted and non-depleted cells of *B. subtilis* IH9016 (P*spac-prsA pbpA-myc cssS::spec*) by immunoblotting with anti-Myc antibodies and the proportion of correctly folded PBP2a-Myc by Bocillin-FL labeling (Zhao *et al*., 1999). Similar quantitation was also performed with the strain *B. subtilis* IH8266 (P*spac-prsA cssS::spec*) and anti-PBP2a antibodies. IH8266 expresses wild-type PBP2a instead of PBP2a-Myc.

The quantitation was performed with a series of twofold diluted membrane samples analysed by SDS-PAGE (Fig. S4). It was observed that the level of Bocillin-FL-binding, correctly folded full-length PBP2a-Myc and PBP2a were decreased by 27–40% in PrsA-depleted cells as compared with non-depleted cells. This indicates that PBP2a misfolding occurs in the absence of PrsA.

Peptidoglycan cross-linkage degree is decreased and amount of muropeptides with pentapeptide chain is increased in cells depleted of PrsA

To elaborate the cell wall defect caused by the PrsA depletion, we performed a muropeptide analysis of cell walls isolated from PrsA-depleted and non-depleted cells of IH7211 (P*spac-prsA*) and the wild-type strain RH2111. Peptidoglycan was extracted from the cells in the late stationary phase as described in *Experimental procedures* and reduced muropeptides were analysed by RP-HPLC. The muropeptide profile consisted of 37 peaks, which were analysed by MALDI-TOF mass spectrometry (Table 1).

At a low level of PrsA (P*spac-prsA* induced with 8 μM IPTG) the amount of muropeptides with pentapeptide chain was significantly increased ($P < 0.0001$) as compared with that in RH2111 with the wild-type level of PrsA (Table 2). The induction of P*spac-prsA* expression in IH7211 with 1 mM IPTG restored a value close to that of the wild-type strain. The PrsA level obtained with the induction is about 60% of the wild-type PrsA level (Vitikainen *et al*., 2001). The cross-linkage degree was significantly decreased ($P < 0.05$) by 2% in the PrsA-depleted cells compared with the wild-type strain (Table 2) and was restored to the wild-type level by the induction of P*spac-prsA* with 1 mM IPTG. Thus, we conclude that the observed differences for peptidoglycan structure are caused by the PrsA depletion.

Van-FL imaging of the cell wall defect of prsA *mutants*

The cell wall defect was further characterized by imaging peptidoglycan biosynthesis in the *prsA* null mutant and PrsA-depleted cells of *B. subtilis* IH7211 with a fluorescent vancomycin (Van-FL). Van-FL binds to the terminal D-Ala-D-Ala moieties in non-cross-linked peptidoglycan precursors and growing glycan chains (Daniel and Errington, 2003; Tiyanont *et al*., 2006). It has been shown by using Van-FL staining and fluorescence microscopy that lateral wall peptidoglycan polymers are synthesized in distinct spots organized in a spiral pattern (Daniel and Errington, 2003; Tiyanont *et al*., 2006). PBPs that are located in the lateral wall in a similar spiral organization pattern are responsible for the synthesis of the lateral wall peptidoglycan. On the other hand, PBPs that normally synthesize the division septum are also capable of synthesizing lateral wall peptidoglycan (Daniel and Errington, 2003).

In cells of *B. subtilis* 168 and IH7211 (P*spac-prsA*) induced with 1 mM IPTG, fluorescence was mainly seen in the division septum (Figs 4D and 5C, right panels, respectively), but the spiral synthesis pattern of lateral wall peptidoglycan was also observed particularly in the case of exponential-phase cells of *B. subtilis* 168 (Fig. 4D). The *prsA* null mutant and PrsA-depleted cells of IH7211 (8 μM and 16 μM IPTG) were more intensively fluorescent than wild-type and non-depleted cells. In thick rods and spherical severely PrsA-depleted cells, fluorescence was strongly increased in the entire wall. As compared with the fairly moderate effect of severe PrsA depletion on the cross-linkage index, only 2%, the strong diffuse Van-FL fluorescence is surprising. This result may suggest that peptidoglycan (lipid II) precursors are more abundant in the membrane of PrsA-depleted than non-depleted cells and distributed evenly around whole deformed cells. Stationary-phase cells of the *prsA* null mutant, including the small cocci-like ones (Fig. 4B and

Table 1. Muropeptide structures and quantification from peptidoglycan of *B. subtilis* RH2111 and conditional mutant IH7211 (P_{spac}-*prsA*) cultured with 8 μM or 1 mM IPTG.

Peak number[a]	Proposed structures[b,c]	Amount of muropeptides (%)[d] RH2111	IH7211 8 μM IPTG	IH7211 1 mM IPTG
1	ds-tri	2.65	1.26	2.63
2	ds-tri (deAc)	0.53	1.00	0.53
3	ds-tri with 1 amidation	10.58	13.39	10.84
4	ds-tri (deAc) with 1 amidation	2.07	1.70	1.70
5	ds-tetra	0.32	0.31	0.22
6	ds-tetra with 1 amidation	0.22	0.33	0.26
7	ds-di	1.39	1.73	1.62
8	ds-tetra with 1 amidation	0.75	1.02	0.71
9	ds-tri-di with 2 amidations	1.06	1.85	1.25
10	ds-tetra with 2 amidations	0.85	0.83	0.82
11	ds-tri-tetra with 2 amidations	0.44	0.22	0.53
12	ds-penta with 1 amidation	0.39	0.95	0.33
13	ds-tri-ds-tetra with 1 amidation and missing GlcNac	1.34	1.19	1.68
14	ds-tri-ds-tetra	1.44	0.80	1.16
15	ds-tetra-tetra with 1 amidation	0.32	0.27	0.28
16	ds-tri-ds-tetra with 1 amidation	8.78	6.63	10.51
17	ds-tri-ds-tetra with 2 amidations and missing GlcNac	0.66	1.43	0.86
18	anhydro ds-tri with 1 amidation	0.10	0.17	1.23
	ds-tri-ds-tetra (deAc) with 1 amidation	2.29	0.86	1.23
19	ds-tri-ds-tetra (deAc) with 1 amidation	1.15	0.69	1.06
20	ds-tri-ds-tetra with 1 amidation	1.89	1.31	2.12
21	ds-tri-ds-tetra with 2 amidations	26.34	30.79	26.32
22	ds-tri-ds-tetra (deAc) with 2 amidations	7.90	6.87	6.04
23	ds-tri-ds-tetra (deAc) with 2 amidations	5.26	4.81	4.37
24	ds-tri-ds-tetra (deAc × 2) with 2 amidations	1.69	1.22	1.15
25	ds-tetra-ds-tetra with 2 amidations	0.87	1.08	0.91
26	ds-penta-ds-tetra with 1 amidation	0.49	0.59	0.38
27	ds-penta-ds-tetra with 2 amidations	1.63	1.95	1.41
28	ds-tetra-ds-tetra with 3 amidations	0.18	0.12	0.19
	ds-tri-ds-tetra-ds-tetra with 3 amidations	0.18	0.12	0.19
29	ds-penta-ds-tetra (deAc) with 2 amidations	0.68	0.83	0.54
30	ds-tri-ds-tetra +Ac with 2 amidations	0.51	0.20	0.59
	ds-tri-ds-tetra-ds-tetra with 2 amidations	0.51	0.20	0.59
31	ds-tri-ds-tetra-ds-tetra with 2 amidations	2.20	1.38	2.95
32	ds-tri-ds-tetra-ds-tetra with 3 amidations	6.01	6.01	6.67
33	ds-tri-ds-tetra-ds-tetra (deAc) with 3 amidations	3.30	2.27	2.77
34	ds-tri-ds-tetra-ds-tetra (deAc × 2) with 3 amidations	1.18	0.66	1.05
35	ds-penta-ds-tetra-ds-tetra with 3 amidations	0.48	0.41	0.46
36	anhydro ds-tri-ds-tetra with 2 amidations	0.78	1.67	0.80
37	anhydro ds-tri-ds-tetra with 2 amidations	0.24	0.38	0.53
	ds-tri-ds-tetra-ds-tetra-ds-tetra with 4 amidations	0.37	0.46	0.53

a. Peak numbers refer to the different peaks separated by RP-HPLC from the muropeptide digest of *B. subtilis* peptidoglycan.
b. Proposed structures according to the masses determined by Maldi-Tof and to the identifications by Atrih *et al.* (1999).
c. ds, disaccharide (GlcNAc-MurNAc); tri, tripeptide (L-Ala-D-Glu-mDAP); tetra, tetrapeptide (L-Ala-D-Glu-mDAP-D-Ala); penta, pentapeptide (L-Ala-D-Glu-mDAP-D-Ala-D-Ala); mDAP, meso-diaminopimelic acid; deAc, deacetylated; +Ac, acetylated.
d. Percentage of each peak was calculated as the ratio of the peak area over the sum of areas of all the peaks identified in the table. The values presented are the mean values obtained on three independent experiments for each strain.

C), were less fluorescent than the deformed exponential-phase cells.

PrsA-dependent membrane proteins as revealed by membrane proteome analysis

The instability of several PBPs in the absence of PrsA suggests that PrsA facilitates the folding of membrane proteins which have a large 'periplasmic' hydrophilic domain(s). In order to identify the PrsA-dependent membrane proteins, membrane proteome analysis of IH7211 (P*spac-prsA*) was performed by using metabolic labeling of PrsA-depleted and non-depleted cells with $^{14}N/^{15}N$ and mass spectrometric quantification of the changes in relative amounts of peptides derived from the labeled proteins (see *Experimental procedures* for methodological details). The proteome analysis consisted of two biological replicates (M1 and M2a) and a technical replicate of the experiment M2a (M2b). With the minimum criterion of two identified peptides, 192 different proteins could be quan-

Table 2. Relative amounts of monomers, dimers, trimers and tetramers and of the different peptide side-chains with a free carboxyl group (acceptor chain) in the peptidoglycan of the different strains.

	Amount of muropeptides (%)[b]		
Muropeptides[a]	RH2111	IH7211 8 μM IPTG	IH7211 1 mM IPTG
Monomers	19.8	22.7	20.9
Dimers	65.9	65.8	63.9
Trimers	13.9	11.1	14.7
Tetramers	0.4	0.5	0.5
Cross-linkage degree	42.5 (0.9)	40.6 (0.7)	42.1 (0.7)
Dipeptide	1.4 (0.1)	1.7 (0.2)	1.6 (0.2)
Tripeptide	51.4 (0.5)	51.7 (0.4)	51.9 (0.2)
Tetrapeptide	2.8 (0.5)	3.2 (0.1)	2.7 (0.3)
Pentapeptide	2.0 (0.1)	2.8 (0.1)	1.7 (0.1)

a. The cross-linkage degree and the relative amounts of the different peptide side-chains were calculated according to Glauner *et al.* (1988).
b. Percentages presented are the mean values of three independent determinations for each strain according to muropeptide structure determination presented in Table 1. Values in brackets are standard deviations.

tified which were predicted to contain transmembrane helices or signal peptides. A majority of them were predicted to be membrane-localized proteins (157–171, depending on the algorithm used), either integral membrane proteins or lipoproteins, but also some established or likely exported/cell wall-associated proteins were identified (the proteins and their predicted subcellular localizations are listed in Table S1).

In PrsA-depleted cells, i.e. P*spac-prsA* induced with 2 μM IPTG, the level of PrsA protein was about 10% of that in non-depleted cells, i.e. P*spac-prsA* induced with 1 mM IPTG (Table 3). The levels of PBP2b, PBP3 and PBP4 were decreased (log2 ratio < –1) in PrsA-depleted cell membranes (Table 3), consistent with the Bocillin-FL labelling and immunoblotting results above. Their amount was 30–40% of that in non-depleted cells and the decrease was observed in the both biological replicates as well as in the technical replicate. Furthermore, the level of PBP2a was decreased in M2a (Table 3). Peptides derived from PBP1a/b, PBP2c, PBP5 and PbpX were also quantified, but their levels were not significantly changed by PrsA depletion. Only a few other proteins were quantified decreased, most notably the bacteriophage SPP1 adsorption protein YueB, which was strongly decreased in all three replicates, being at the lowest only 15% of the level of the PrsA-expressing cells in M2a (Table 3). Transmembrane topology prediction of YueB (TMHMM) suggests that it has membrane-spanning segments close to the N- and C-termini and between them a large 'periplasmic' domain (about 900 amino acids). The reduced amount of YueB protein at a low level of PrsA suggests that this domain folds in a PrsA-dependent manner. The levels of OxaA2, ComE and YvrA proteins were slightly decreased in one or two of the replicates. The proteome analysis also suggested that some proteins were more abundant in PrsA-depleted membranes than in non-depleted ones. Among them are the WapA wall-associated protein and the LytA membrane protein, which were detected at about twofold higher levels in two of the replicates (Table S1).

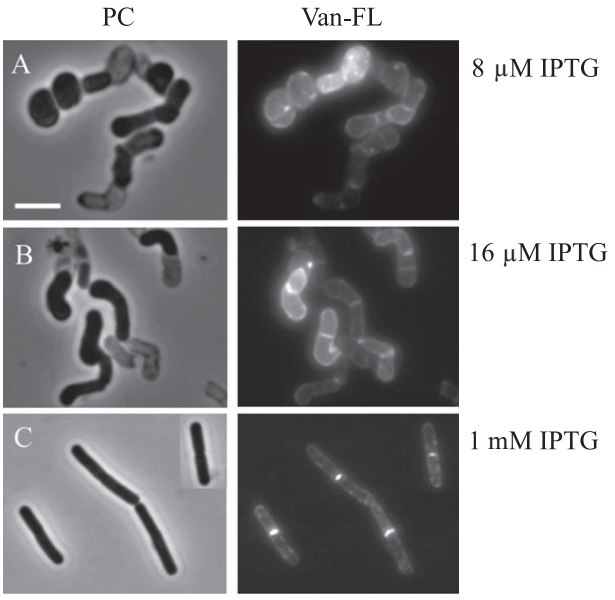

Fig. 5. Van-FL staining of *B. subtilis* strain IH7211 (P*spac-prsA*). Left panels – phase contrast images, right panels – Van-FL staining. P*spac-prsA* expression was induced with IPTG as indicated. Scale bar represents 6 μm (the same for all the images).

PrsA is localized in spots with a spiral-like pattern of organization along the cell membrane

In order to find out whether the PrsA lipoprotein is distributed evenly around the cell membrane or in an uneven manner like MreC and several PBPs, we constructed the *B. subtilis* IH8478 strain which expresses PrsA modified with a C-terminal Myc-tag. This strain was subjected to a procedure (see *Experimental procedures*) in which PrsA-

Table 3. Decreased levels of membrane proteins with a large 'periplasmic' domain in PrsA-depleted cells.

		M1				M2a				M2b			
Gene names	Protein Names	Weighted average ratio (given by CENSUS)	Normalized Ratio	log2[a] RATIO	Number of quantified Peptides	Weighted average ratio (given by CENSUS)	Normalized Ratio	log2[a] RATIO	Number of quantified Peptides	Weighted average ratio (given by CENSUS)	Normalized Ratio	log2[a] RATIO	Number of quantified Peptides
prsA	Foldase protein PrsA	0.12	0.12	–3.01	12	0.16	0.13	–2.90	11	0.15	0.12	–3.11	6
pbpB	Penicillin-binding protein 2b	0.32	0.32	–1.64	5	0.41	0.34	–1.55	10	0.39	0.30	–1.73	7
pbpC	Penicillin-binding protein 3	0.40	0.41	–1.30	8	0.41	0.34	–1.55	17	0.41	0.32	–1.66	10
yueB	Bacteriophage SPP1 adsorption protein YueB	0.44	0.44	–1.18	2	0.18	0.15	–2.73	12	0.26	0.20	–2.31	10
pbpD	Penicillin-binding protein 4	0.46	0.47	–1.09	3	0.48	0.40	–1.32	6	0.49	0.38	–1.40	6
comEA	ComE operon protein 1	0.83	0.84	–0.25	3	0.53	0.44	–1.18	2	0.94	0.73	–0.46	2
oxaA2	Membrane protein OxaA 2	1.79	1.81	0.85	2	0.45	0.38	–1.41	4	0.48	0.37	–1.43	4
yvrA	YvrA	0.75	0.76	–0.39	5	0.69	0.58	–0.80	6	0.60	0.46	–1.11	3
pbpA	Penicillin-binding protein 2a					0.41	0.34	–1.55	2	0.75	0.58	–0.78	3

a. The shading shows more than 2-fold decreased levels.

Myc was stained with anti-c-Myc antibodies, secondary antibodies conjugated with biotin and ExtrAvidin conjugated with Cy3. The stained PrsA-Myc was visualized by fluorescence microscopy. The localization pattern of PrsA-Myc was determined both in cells from the exponential and stationary phase of growth. To show specific binding of the antibodies, *B. subtilis* strain 168 (RH2111) was used simultaneously as a negative control. Indeed, no Cy3 signal was detected in the control strain (see Fig. S5).

The fluorescence images showed that PrsA is not distributed evenly in the membrane but it is localized in distinct spots that are lined up in spirals (Fig. 6). This pattern is stable throughout vegetative growth until stationary phase. However, the spiral structures are better resolved in exponentially growing cells than in stationary phase cells.

PrsA is an oligomeric protein

It has been shown that MreC is a dimeric protein and this structure may be important for its putative function as a scaffold for recruiting PBPs and spatially organizing the lateral cell wall synthesis (van den Ent *et al*., 2006). We used formaldehyde cross-linking of PrsA and PrsA-Myc in whole cells and immunoblotting with anti-c-Myc and anti-PrsA antibodies to study whether PrsA is a monomeric or dimeric/multimeric protein. The non-random localization pattern suggests that PrsA may be associated with some other protein(s) which has the same or similar localization pattern, e.g. MreC or some of the PBPs. The cross-linking approach might also reveal such interactions.

The cross-linking of cells expressing either wild-type PrsA or PrsA-Myc revealed, in addition to the 33 kDa PrsA or PrsA-Myc monomers, two other PrsA-containing bands of higher molecular weights, one migrating (in SDS-PAGE) at approximately 65 kDa and the other one slightly above it (~68 kDa) (Fig. 7). The 65 kDa form was very heat resistant; it did not disappear at heating for 30 min at 95°C and analysis in SDS-PAGE in the presence or absence of dithiotreitol (Fig. 7 and data not shown). A small amount of this protein could also be detected in non-cross-linked cells. The molecular weight suggests that it might be a PrsA dimer. Consistently, *B. subtilis* PrsA expressed in and purified from *E. coli* contained this same form and its amount increased by cross-linking of the purified PrsA. The 68 kDa band was detected only in lanes containing cross-linked *B. subtilis* cell or PrsA protein (from *E. coli*) samples and it disappeared by heating at 95°C. It most probably contains oligomeric PrsA which migrated clearly faster than what is expected for PrsA trimers or tetramers. A few very weak bands of high-molecular-weight complexes (> 68 kDa) were also detected, but further studies are needed to elucidate

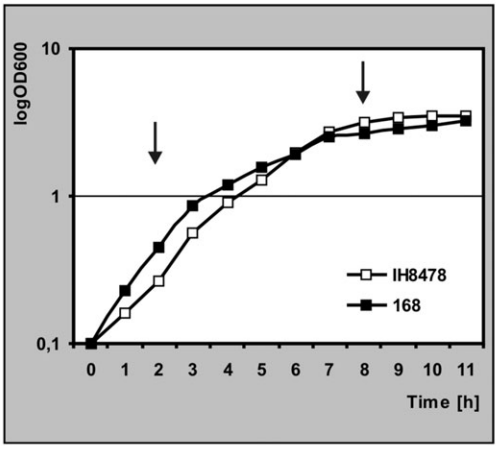

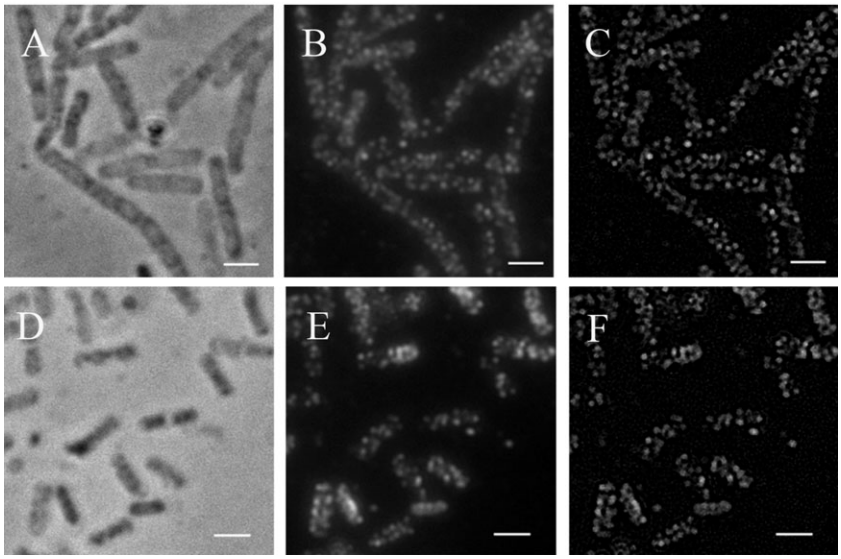

Fig. 6. Immunolocalization of PrsA-Myc in *Bacillus subtilis* IH8478 strain in exponential (A–C) and stationary phase (D–F). Immunostaining has been described in *Experimental procedures*. Scale bar – 2 μm. The upper panel shows growth curves of *B. subtilis* IH8478 and *B. subtilis* 168, the parental strain which does not express PrsA-Myc. Arrows indicate time points when samples were collected for immunofluorescence microscopy.
A. and D. Phase contrast pictures.
B. and E. Fluorescence pictures of Cy3-stained cells.
C. and F. Fluorescence pictures after deconvolution.

whether they contain PrsA associated with some other components of the membrane/wall.

Small-angle X-ray scattering (SAXS) was another method to elucidate the multimeric structure of PrsA (Rodgers *et al*., 1996). *Escherichia coli*-produced PrsA protein was subjected to SAXS and the radius of gyration (*Rg*) was determined. PrsA had the Rg of 27–29 Å (Fig. S6), which further suggests that PrsA forms oligomers.

Discussion

PrsA peptidyl-prolyl *cis-trans* isomerase has an essential role in extracytoplasmic protein folding in rod-shaped bacteria. The localization of the enzyme domain at the membrane-cell wall interface suggests that PrsA may assist the folding of membrane proteins which have large functional domains on the outer surface of the membrane. In this study we used several methodological approaches to identify membrane proteins which are dependent on PrsA for folding with the emphasis on identifying the PrsA-dependent component(s) that is (are) involved in cell shape determination and/or cell wall synthesis.

PrsA is most probably involved in lateral cell wall biosynthesis of *B. subtilis* as suggested by the morphological changes in the absence of PrsA. Severely PrsA-depleted cells are spherical in shape and pearl necklace-like round-cell chains are formed, but a high concentration of magnesium probably stabilizes peptidoglycan enabling the bacterium to maintain its rod shape (thick) at very low PrsA levels. Consistently also small cocci-like cells were formed in stationary phase cultures of the *prsA* null mutant. In the wild type-like rods of the *prsA* null mutant, the lateral wall synthesis may have been restored by some compensation mechanism for instance a secondary suppressor mutation.

Our results suggest that PrsA is required for lateral cell wall biosynthesis as the folding and stability of those PBPs which are involved in the lateral wall synthesis are

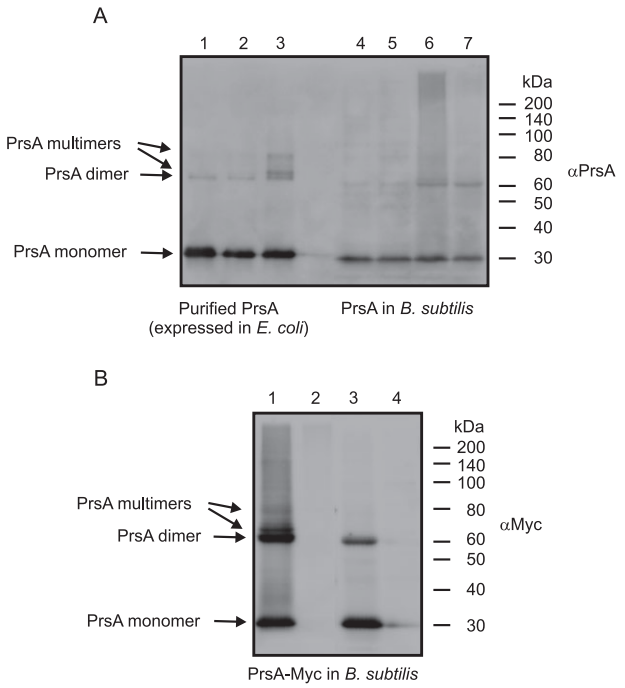

Fig. 7. PrsA dimers and oligomers as revealed by formaldehyde cross-linking of whole *B. subtilis* cells and purified PrsA. Cross-linked PrsA (A) or PrsA-Myc (B) complexes were detected by immunoblotting.
A. Non-lipomodified PrsA expressed in the cytoplasm of *E. coli* and purified (lanes 1–3) and lipomodified PrsA in whole cells of *B. subtilis* RH2111 (lanes 4–7). Heating of non-cross-linked (lanes 1, 2, 4 and 5) or cross-linked (lanes 3, 6 and 7) samples in SDS-PAGE sample buffer at 37°C for 10 min (lanes 1, 3, 4 and 6) or at 95°C for 30 min in the presence of 10 mM dithiothreitol (lanes 2, 5 and 7).
B. Lipomodified PrsA-Myc in *B. subtilis* IH8478 cross-linked and heated at 37°C for 10 min (lane 1) or at 95°C for 30 min (lane 3). Corresponding samples from *B. subtilis* RH2111, the parental strain not expressing PrsA-Myc, were used as negative controls (lanes 2 and 4 respectively).

dependent on PrsA. Levels of several high-molecular-weight PBPs (PBP2a, PBP2b, PBP3 and PBP4) were significantly decreased in PrsA-depleted cells, in contrast to some other proteins (MreC and PBP1a/b) located in the same compartment. We could also demonstrate that misfolding of PBP2a occurred in the absence of PrsA and the misfolded PBP2a was degraded in a manner dependent on the CssRS two-component system. It seems that PrsA is required either directly or indirectly for PBP2a folding, and most probably also for the folding of the other PrsA-dependent PBPs, and the primary reason for the growth inhibition and cell wall synthesis defect is probably insufficient amount of active PBPs. Most likely HtrA and HtrB proteases are involved in the degradation of misfolded PBP2a, as CssRS is a dedicated regulator of their expression (Hyyrylainen *et al.*, 2005). HtrA/DegP-type proteases have in addition to the proteolytic activity a chaperone activity which catalyses protein folding (Spiess *et al.*, 1999; Antelmann *et al.*, 2003) and this may explain the effect of CssRS on the folding of PBP5. Our results suggest that PrsA and CssRS have an overlapping and redundant role in the folding of PBP5, but further work is needed to characterize the interplay of these components at the molecular level in detail.

Severe PrsA depletion decreased the cross-linkage degree but only by 2%. This is surprising as cells are spherical or large rods in severely PrsA-depleted cultures. PBPs that normally synthesize the division septum, particularly PBP1a/b, which was stable in PrsA-depleted cells, may have taken a larger role in the cross-linkage/synthesis of the whole cell wall peptidoglycan. This would explain the relatively moderate decrease in the cross-linkage index. The peptidoglycan structure is only moderately impaired, but the bacterium is spherical in shape. In contrast to wild-type cells, Van-FL stained strongly Δ*prsA* and PrsA-depleted exponential-phase cells and the fluorescence was fairly uniformly distributed around the whole cell membrane. The increased number of remaining pentapeptide side-chains and their even distribution in the wall might explain the increased Van-FL staining. However, the fairly moderate effect of PrsA-depletion on the peptidoglycan structure may not be consistent with this explanation. An alternative hypothesis might be that the level of membrane-bound peptidoglycan precursors was increased in these deformed cells and that the precursors either moved freely in the membrane or were translocated uniformly across the membrane.

Does PrsA assist directly PBP folding or is the effect indirect i.e. via catalysis of folding of a third component which influences PBP folding? We tried to demonstrate *in vitro* with purified PBP2a and PrsA a direct role for PrsA in the catalysis of PBP2a folding by measuring the folding kinetics of denatured PBP2a with the binding of Bocillin-FL, but it did not succeed. The result was very similar as previously with AmyQ α-amylase: the denatured protein folded rapidly to correct enzymatically active conformation and independently of PrsA. In the compartment at the membrane-wall interface ('periplasm'), AmyQ folding is strongly dependent on PrsA, but in protoplasts in the absence of the wall AmyQ folds independently of PrsA (Hyyryläinen *et al.*, 2001; Vitikainen *et al.*, 2001; Wahlstrom *et al.*, 2003). Thus, the folding assistance requirement is dependent on the cell wall environment. The situation with PBP2a and other PrsA-dependent PBPs is probably very similar. PrsA assistance is needed for folding in the 'periplasm' only. PBPs, and also AmyQ, are fairly large proteins and have numerous proline residues. Therefore, it is likely that direct assistance of chaperones and foldases is needed for their folding in the cell wall environment. Why is then PBP1a/b independent of PrsA? It is a larger protein than the other PBPs and AmyQ. One explanation could be that in addition to PrsA and CssRS

(HtrA/B), which both are involved in PBP5 folding, a third chaperone catalyses PBP1a/b folding.

A wider search for PrsA-dependent proteins was performed by analysing PrsA-dependent changes in membrane proteome by mass-spectrometry. The proteome analysis suggested that PPB2a, PBP2b, PBP3 and PBP4 are the main PrsA-dependent proteins in the membrane. In addition to them, only a few other membrane proteins exhibited decreased stability in PrsA-depleted cells, most significantly the SSP1 receptor YueB. This fairly small set of PrsA-dependent proteins supports a direct rather than an indirect effect of PrsA on PBP folding. One can envision an indirect effect if PrsA determines the isomeric state of a prolyl bond in a third component, e.g. MreC, the stability of both these conformers is similar and the position of the prolyl switch affects the folding and stability of PBPs.

Despite of the rod cell shape, *Corynebacteria* such as *C. glutamicum* and *Corynebacterium diphtheriae*, which belong to the Actinobacteria group of Gram-positive bacteria, do not possess PrsA (Kalinowski *et al*., 2003). Obviously they do not need a PrsA-like foldase/chaperone to synthesize the lateral wall and maintain the rod cell shape. The PrsA-independency may be due to the different mode of lateral wall synthesis in these bacteria as compared with *B. subtilis* and most probably other rod-shaped Firmicutes; it has been shown that in *C. glutamicum* peptidoglycan is incorporated into the wall via cell poles in a manner dependent on the DivIVA protein (Daniel and Errington, 2003; Letek *et al*., 2008). PrsA is also a dispensable protein in cocci (Drouault *et al*., 2002; Ma *et al*., 2006). Because in cocci peptidoglycan is assembled at the division septum and the hemispherical poles derived from it (Pinho and Errington, 2003), the same reason may explain why PrsA is dispensable in them.

In *B. subtilis*, the DivIB, DivIC and FtsL cell division proteins and the PBP 2b form a protein complex that assembles in an interdependent manner (Daniel *et al*., 2006). It has also been shown that FtsL and DivIC are unstable in cells depleted of PBP2b (Daniel *et al*., 2006). FtsL is a particularly unstable protein in the absence of the interacting proteins (Bramkamp *et al*., 2006). PBP2b was one of those PBPs which were degraded in the absence of PrsA and this could affect the stability of the whole complex. Therefore, we studied the effect of PrsA depletion on the stability of the divisome proteins by using N-terminal GFP fusions of these proteins. Surprisingly, their stability was independent of the expression of PrsA in this assay. The membrane proteome analysis of PrsA-depleted cells also showed a clear decrease in the level of PBP2b but no effect on the level of DivIB; FtsL and DivIC could not be detected. An NMR study has shown that the DivIB protein of *Geobacillus stearothermophilus* is in two distinctly different conformations depending on the *cis-trans* isomerization of a Tyr-Pro peptide bond in the extracytoplasmic β-domain and it was speculated that the *cis-trans* isomerization may modulate the assembly of the divisome complex (Robson and King, 2006). Our finding that PrsA depletion has no effect on the stability of DivIB, DivIC and FtsL does not support the hypothesis about a regulatory role of *cis-trans* isomerization in the divisome complex assembly in *B. subtilis*.

We also determined the localization of PrsA in the membrane by taking advantage of a *B. subtilis* strain that expresses Myc-tagged PrsA. Because the *prsA-myc* fusion gene is present as a single copy in the chromosome and under the control of the native *prsA* promoter, artefacts due to overproduction were avoided. The results showed that PrsA is not randomly distributed in the membrane. It (PrsA-Myc) was localized to the lateral cell membrane in which it formed distinct spots organized in a helical pattern. To our knowledge this is the first lipoprotein which has been shown to have the helical organization pattern. Still little is known about the mechanism underlying helical distribution of proteins along the membrane. The helical organization of PrsA raises the question whether it is associated with any of the other proteins with the similar organization pattern including the cytoskeleton proteins and PBPs. The helical pattern might be dependent on them. It has been shown that a cytoskeleton protein (MreBH) can determine the helical organization of a protein (LytE) on the extacytoplasmic side of the membrane (Carballido-Lopez *et al*., 2006). We also demonstrated that PrsA forms dimers/oligomers, but the functional significance of the dimeric/oligomeric structure is still unclear.

PrsA foldase/chaperone catalyses post-translocation folding of exported proteins (Jacobs *et al*., 1993; Hyyryläinen *et al*., 2001; Vitikainen *et al*., 2004). It has been shown that overexpression of PrsA over the wild-type level enhances secretion of some extracellular proteins particularly α-amylases of *Bacillus* sp. from industrial Gram-positive bacteria (Kontinen and Sarvas, 1993; Vitikainen *et al*., 2001, 2005; Williams *et al*., 2003; Lindholm *et al*., 2006). Therefore, PrsA is an important tool for increasing yields in industrial protein production especially thermoresistant α-amylases for various applications needing degradation of starch to smaller sugars, including bioethanol production. Now we have shown that PrsA also has a housekeeping role in the cell. It is required directly or indirectly for PBP folding and lateral cell wall biosynthesis. A class of most important current antibiotics, β-lactams, exerts the antimicrobial effect by inhibiting PBPs. Our results suggest that inhibiting PrsA might be an alternative and additive way to inhibit cell wall biosynthesis of pathogenic rod-shaped bacteria and treat infectious diseases. PrsA-targeted antimicrobials could also inhibit bacterial pathogenesis by inhibiting secretion of critical virulence factors for instance listeriolysin O and broad-range phospholipase C in *Listeria monocytogenes* (Alonzo *et al*.,

Table 4. *B. subtilis* strains used in this study.

Strain[a]	Relevant genotype	Reference
IH7211	168 *prsA*::pKTH3384 P*spac-prsA*	Vitikainen *et al.*, 2001
IH8266	168 *prsA*::pKTH3384 P*spac-prsA cssS*::*spec*	This study
IH8435	3417 *prsA*::pKTH3384 P*spac-prsA*	This study
IH8437	3103 *prsA*::pKTH3384 P*spac-prsA*	This study
IH8441	2083 *prsA*::pKTH3384 P*spac-prsA*	This study
IH8445	JAH66 *prsA*::pKTH3384 P*spac-prsA*	This study
IH8456	168 Δ*pbpF*::*ery*	This study
IH8458	168 *dacA*::*cat*	This study
IH8460	168 Δ*pbpD*::*ery*	This study
IH8462	168 Δ*ponA*::*spec*	This study
IH8464	168 *pbpC*::*spec*	This study
IH8471	168 *divIC*::pKTH3806 P*xyl-gfp-divIC*	This study
IH8473	168 *divIB*::pKTH3814 P*xyl-gfp-divIB*	This study
IH8478	168 *prsA*::pMUTIN-cMyc *prsA-myc*	This study
IH8480	IH8471 *prsA*::pKTH3384 P*spac-prsA*	This study
IH8483	IH8473 *prsA*::pKTH3384 P*spac-prsA*	This study
IH8999	168 *pbpA*::*ery*	This study
IH9003	168 *pbpA*::pKTH3828 *pbpA-myc*	This study
IH9013	IH9003 *cssS*::*spec*	This study
IH9016	IH9013 *prsA*::pKTH3384 P*spac-prsA*	This study
IH9024	168 Δ*prsA*	This study
IH9025	168 *dacA*::pKTH3831 *dac-myc*	This study
IH9027	IH9003 *prsA*::pKTH3384 P*spac-prsA*	This study
IH9028	IH9025 *prsA*::pKTH3384 P*spac-prsA*	This study
IH9029	IH9028 *cssS*::*spec*	This study
2083 (RH2225)	168 *ponA*::pSG1492 P*xyl-gfp-ponA*	Scheffers *et al.*, 2004
3103 (RH2227)	168 *pbpA*::pSG5043 P*xyl-gfp-pbpA*	Scheffers *et al.*, 2004
3417 (RH2224)	168 *mreC*::pSG5276 P*xyl-gfp-mreC*	Leaver and Errington, 2005
DPVB207 (RH2223)	PS832 Δ*pbpH*::*spec pbpA*::*ery amyE*::P*xyl-pbpH*	Wei *et al.*, 2003
PS1869 (RH2234)	PS832 Δ*pbpF*::*ery*	McPherson *et al.*, 2001
PS1900 (RH2235)	PS832 *dacA*::*cat*	Popham *et al.*, 1996
PS2022 (RH2236)	PS832 Δ*pbpD*::*ery*	Popham and Setlow, 1996
PS2062 (RH2237)	PS832 Δ*ponA*::*spec*	McPherson *et al.*, 2001
PS2328 (RH2238)	PS832 *pbpC*::*spec*	Wei *et al.*, 2003
PS832	Wild type, Trp$^+$ revertant of 168	Wei *et al.*, 2003
168 (RH2111)	*trpC2*	Kunst *et al.*, 1997
JAH66 (RH2229)	1012 *amyE*::*gfp-ftsL*	Heinrich *et al.*, 2008

a. In parenthesis are shown the strain codes in the collection of THL.

2009; Zemansky *et al.*, 2009). Because human and other eukaryotic cells also have functionally important parvulin-type PPIases, PrsA inhibitors should be PrsA specific. The designing of PrsA inhibitors could take advantage of structural and mechanistic differences between bacterial and eukaryotic parvulins (Heikkinen *et al.*, 2009). We can envision that such PrsA inhibitors could either inhibit specifically the PPIase activity or interfere with functions of the N- or C-terminal domains, which may be chaperone or interaction domains. Alternatively, eukaryotic cell membrane could be impermeable to PrsA inhibitors.

Experimental procedures

Bacterial strains, plasmids and growth conditions

Bacillus subtilis strains and plasmids used in this study are listed in Table 4 and Table S2 respectively. *Escherichia coli* DH5α was used for cloning. Bacteria were grown in LB or TY medium and on corresponding agar plates at 37°C, but also some other culture media were used for particular experiments. The metabolic labelling for membrane proteome analysis was performed with cells grown in a synthetic minimal medium (BMM) (Stulke *et al.*, 1993). Cultivations were performed in Antibiotic Medium 3 when the effect of magnesium on PrsA-depleted cells and Van-FL staining of peptidoglycan synthesis in *prsA* null mutant were studied. The growth media were supplemented with appropriate antibiotics when needed to maintain plasmids and chromosomal plasmid integrants in the cells. The antibiotics (and their concentrations) used in the cultivations were ampicillin (100 μg ml^{-1}), erythromycin (0.5, 1 or 100 μg ml^{-1}), lincomycin (12.5 μg ml^{-1}), chloramphenicol (5 μg ml^{-1}) and spectinomycin (100 μg ml^{-1}). The expression of P*spac-prsA* was induced with 1 mM (full induction) or with 0, 2, 8, 16 or 24 μM (PrsA depletion) IPTG. For the PrsA depletion experiments, bacteria were taken from fresh agar plates, washed several times in LB medium and then used to inoculate the cultures. The expression from P*xyl* was induced with 0.5% xylose.

Plasmid constructions

To construct pKTH3805, a fragment of the coding region of *prsA* (bp 633–938) was PCR-amplified with the primers prsAmyc-fw (5′cacaggtaccatggacgaaacattcagcaaag) and prsAmyc-rv (5′cacacggccgtttagaattgcttgaagatgaagaagtg). The amplified fragment was inserted into the pGEM-T-Easy vector (Promega). The recombinant plasmid was digested with KpnI and EagI, the released *′prsA* fragment was ligated with pMUTIN-cMyc (Kaltwasser *et al*., 2002) cut with the same restriction enzymes and the ligation mixture was used to transform competent *E. coli* DH5α cells. The obtained plasmid carrying the *′prsA* fragment (pKTH3805) was used to transform *B. subtilis* RH2111 (168). The Campbell-type integration of pKTH3805 into the *prsA* gene resulted in the formation of *prsA-myc*, which encodes PrsA bearing a C-terminal Myc-tag. The chromosomal integration of pKTH3805 replaced the wild-type *prsA* with *prsA-myc*. The viability of the resulted strain *B. subtilis* IH8478 indicates that PrsA-Myc is functional.

Bacillus subtilis IH9003 expressing *pbpA-myc* was constructed by transforming 168 with plasmid pKTH3828. This plasmid was constructed by PCR-amplifying a *′pbpA-myc* fragment with the primers pbpA-fw (5′cacaggatccatagcaaatggtggctaccgc) and pbpA-rv (cacagtcgacttacagatcttcttcgctgatcagtttctgttcgttatcagaagacgttgtgttttctgc) and inserting the fragment between the BamHI and SalI sites of the pSG4902 plasmid (Scheffers *et al*., 2004). The Campbell-type integration of pKTH3828 into the *pbpA* gene resulted in the formation of *pbpA-myc*.

Bacillus subtilis IH9025 expressing *dacA-myc* was constructed in a similar manner as *B. subtilis* IH9003. The *′dacA-myc* fragment in pKTH3831 was PCR-amplified with the primers dacA-fw (5′cacagtcgacggaacagctgaacgcaacg) and dacA-rv (5′cacagaattcttacagatcttcttcgctgatcagtttctgttcaaaccagccggttaccgtatc) and inserted between the SalI and EcoRI sites of pSG4902.

To construct pKTH3814, a fragment of the *divIB* gene (bp 295–633) was PCR amplified with the primers divIB-fw (5′cacactcgaggtcatgaacccgggtcaagacc) and divIB-rv (5′cacagaattcaggaagcgatttgctgatctcc). The amplified fragment was inserted between the XhoI and EcoRI sites of the pSG4902 plasmid (Scheffers *et al*., 2004). The resulted pKTH3814 plasmid was used to transform *B. subtilis* RH2111. pKTH3814, upon integration into the *B. subtilis* chromosome, disrupted the native *divIB* gene and created a *gfp-divIB* fusion (*B. subtilis* IH8473), which is expressed from the xylose-inducible P*xyl* promoter.

Bacillus subtilis IH8471 expressing *gfp-divIC* was constructed in a similar manner as *B. subtilis* IH8473. A fragment of the *divIC* gene (bp 455–755) was PCR amplified with the primers divIC-fw (5′cacaggatcccttgaattttccagggaacga) and divIC-rv (5′cacactcgaggacgtaatcctcatccttcaatttg). The *′divIC* fragment was cloned in the pGEM-T-Easy vector. The fragment was released by digesting with BamHI and XhoI, and inserted into pSG4902. *Bacillus subtilis* RH2111 was transformed with the obtained plasmid, pKTH3806.

Construction of the prsA null mutant

Chromosomal DNA was isolated from *B. subtilis* IH7075 (in the culture collection of THL) and used to transform *B. subtilis* 168 (RH2111). In IH7075, the *prsA* gene is deleted and replaced with the *cat* gene from pC194. The IH7075 strain also harbours plasmid pKTH3327, which carries *prsA* under the control of the P*spac* promoter and complements the chromosomal *prsA* deletion. The Δ*prsA* mutation deletes the coding sequence of *prsA*, and 153 bp and 75 bp of the up- and downstream regions respectively. The *prsA* null mutants of 168 were selected on Antibiotic Medium 3 –plates containing 20 mM $MgCl_2$ and chloramphenicol (5 μg ml^{-1}).

SDS-PAGE and immunoblot analysis of PrsA, MreC, PBP2a and GFP-fusion proteins

Whole cell samples were prepared from cultures in the late exponential (Klett100 + 1 h) or early stationary (Klett100 + 3 h) phase of growth. Cells were harvested by centrifugation from 1 ml of culture, resuspended in 50 μl of protoplast buffer (20 mM potassium phosphate pH7.5, 15 mM $MgCl_2$, 20% sucrose and 1 mg ml^{-1} lysozyme) and incubated at 37°C for 20 min. Then 50 μl of 2×Laemmli sample buffer was added and the samples were boiled for 10 min at 100°C. Proteins were separated in SDS-PAGE and blotted onto a PVDF nylon filter (Immobilon-P transfer membrane; Millipore). The immunodetection of PrsA, PrsA-Myc, MreC, PBP2a and GFP-fusion proteins was performed using specific antibodies against these proteins (or Myc-tag) and goat anti-rabbit IgG (H + L)-HRP conjugate (Bio-Rad). ECL reactions were performed using an Immun-Star WesternC kit according to the instructions of the manufacturer (Bio-Rad) and proteins were visualized and quantified with a FluorChem HD2 imager and AlphaEase FC software (AlphaInnotech).

Isolation of bacterial cell membranes and Bocillin-FL labelling of penicillin-binding proteins

Bacterial cell membranes were prepared from 500 ml of culture in LB medium. Cells were harvested at the cell density of Klett100 by centrifugation, washed once with potassium phosphate buffer (20 mM potassium phosphate pH 7.5, 140 mM NaCl) and resuspended in the washing buffer. The cells were disrupted by passing the suspension through a French press cell twice at 20 000 lb in^{-2}. The cell lysate was centrifuged at 8000 *g* for 10 min, followed by centrifugation of the supernatant at 217 500 *g* for 1 h. The membrane pellet was resuspended in the phosphate buffer (1 ml). Protein concentrations of the membrane preparations were determined using a 2-D Quant Kit (GE Healthcare) or Micro BCA (Pierce) according to the instructions of the manufacturers.

In the Bocillin-FL labelling reaction, cell membranes (300 μg protein) were treated with 10 μM Bocillin-FL in a final volume of 100 μl. The reaction mixtures were incubated at 35°C for 30 min, followed by addition of 100 μl 2×Laemmli buffer and incubation at 100°C for 3 min. Samples corresponding 15 μg of protein were separated in 10% SDS-PAGE. Fluorescent PBPs were visualized using a fluoroimager Typhoon 9400 (Amersham Biosciences) with excitation at 488 nm and emission at 520 nm. Levels of active Bocillin-FL-labelled PBP2a were quantified with the ImageQuantTL software (Amersham Biosciences).

Peptidoglycan extraction and muropeptide analysis

Bacillus subtilis cells were grown in LB medium, a volume corresponding V × OD = 300 was taken in the late stationary phase (Klett100 + 6 h) and the cells were harvested by centrifugation. Peptidoglycan extraction and muropeptide analysis were performed as described previously for *L. lactis* (Courtin *et al*., 2006). Purified peptidoglycan was digested with mutanolysin (muramidase from *Streptomyces globisporus*; Sigma-Aldrich). Soluble muropeptides were reduced with sodium borohydride as described (Atrih *et al*., 1999) and separated on a Hypersil-100 column (C18, 250 by 4.6 mm, 5 μm; Thermo Finnigan) at 50°C by RP-HPLC. The column was eluted with 10 mM ammonium phosphate pH 4.6 and 0.18% sodium azide for 5 min, followed by a linear gradient of methanol (0–20%) for 270 min as described previously (Courtin *et al*., 2006). Samples of eluted muropeptides were analysed by MALDI-TOF mass spectrometry (Voyager DE STR, Applied Biosystems, Framingham, MA) with α-cyano-4-hydrocinnamic acid matrix. For most fractions, 1 μl of sample was sufficient. For less abundant fractions, 100 μl was concentrated on a ZIP-Tip C18 pipette tip (Millipore) and eluted with 1 μl of solvent (50% acetonitrile and 0.15% trifluoroacetic acid) prior to analysis.

The cross-linkage degree was calculated according to Glauner (1988) with the formula: (1/2 Σ dimers + 2/3 Σ trimers + 3/4 Σ tetramers)/ Σ all muropeptides.

The percentage of muropeptides with a certain side peptide chain (X = di, tri, tetra and penta) with free COOH (donor chain) was calculated according to Glauner (1988).

$$\text{percentage (X)} = \left[\Sigma\ \text{monomers(X)} + \frac{1}{2}\Sigma\text{dimers(X)} + \frac{1}{3}\Sigma\text{trimers(X)} + \frac{1}{4}\Sigma\text{tetramers(X)}\right] \Big/ \Sigma\ \text{all muropeptides.}$$

Statistical analysis of the data was performed with Statgraphics Plus software (Manugistics, Rockville, MD, USA). The results obtained with two strains were compared with a two-sample comparison analysis and a *t*-test.

Van-FL staining and fluorescence microscopy

Bacillus subtilis strains 168 and Δ*prsA* were grown over night in 10 ml of Antibiotic medium 3 (Difco) suplemented with 20 mM MgCl2 and 5 μg ml^{-1} chloramphenicol when needed. Over night cultures were diluted in 20 ml of fresh medium to OD600 = 0.1 and grown 24 h. Cells were collected for Van-FL staining at exponential, stationary and late stationary phases. *Bacillus subtilis* strain IH7211 was grown overnight on a TY agar plate supplemented with 1 μg ml^{-1} erythromycin. Material from plate was suspended in phosphate-buffered saline (PBS) to OD_{600} = 1.0 and washed three times with 1 ml of PBS. 20 μl of the suspension was used to inoculate 10 ml of TY containing 1 μg ml^{-1} erythromycin and IPTG at three different concentrations: 8 μM, 16 μM and 1 mM. At OD_{600} = 0.6, samples were collected for Van-FL staining.

A culture of 0.5 ml was incubated 20 min with 1 μg ml^{-1} fluorescently labelled vancomycin (BODIPY® FL vancomycin, Invitrogen) mixed in 1:1 ratio with unlabelled vancomycin (Sigma). The cells were spotted on microscope slides (Knittel Gläser, Germany). The Van-FL-stained cells were viewed immediately under a fluorescence microscope (Olympus IX71) equipped with a Cool Snap HQ2 camera (Photometrics). Van-FL fluorescence was visualized with a bandpass 470/40 nm excitation filter and a bandpass 525/50 nm emission filter. Images were analysed using ImageJ (http://rsb.info.nih.gov/nih-image/) and Adobe Photoshop CS2 Version 9.0.

Electron microscopy

For electron microscopy, cells were fixed with 2.5% glutaraldehyde overnight at 4°C as has been described (Leaver and Errington, 2005). The fixed cells were washed twice in phosphate buffer and then treated with 1% osmium tetroxide for 1 h. The samples were dehydrated with a series of treatments with ethanol and acetone, followed by embedding in Epon resin. The microscopy was performed in the Institute of Biotechnology, University of Helsinki, by using a JEOL 1200EX II electron microscope.

Quantification of the effect of a minimal PrsA concentration on the membrane proteome of B. subtilis

For metabolic labelling, *B. subtilis* IH7211 (P_{spac}-*prsA*) was grown aerobically at 37°C in a synthetic minimal medium (BMM). The medium was either supplemented with ^{15}N-ammonium sulphate, ^{15}N-L-tryptophan and ^{15}N-L-glutamate (Cambridge Isotope Laboratories, Andover, USA) or ^{14}N-ammonium sulphate, ^{14}N-L-tryptophan and ^{14}N-L-glutamate. Cells from overnight cultures grown with 40 μM IPTG were washed with warm BMM and used to inoculate the cultures for the metabolic labelling. In order to realize two different biological states, 2 μM IPTG was used in the cultivation M1 with the light form of nitrogen source and 1 mM IPTG with the heavy one (see below). A biological replicate (M2a) was performed with identical cultures but the labels were switched. Cells were harvested in the exponential phase of growth and equivalent OD-units of bacteria either grown with ^{15}N-BMM or ^{14}N-BMM were combined in proportion 1:1 and stored at –20°C.

The combined cells were disrupted on ice using a French press cell, followed by separation of cell debris by centrifugation and extraction of cell membranes according to the method described by Eymann and collaborators (Eymann *et al*., 2004). Membranes were centrifuged at 100 000 *g* for 60 min at 4°C, followed by purification steps with high salt buffer [20 mM Tris-HCl, pH7.5, 10 mM EDTA, 1 M NaCl, Complete Protease Inhibitor (Roche)], alkaline Na_2CO_3 buffer (100 mM Na_2CO_3-HCl, pH 11, 10 mM EDTA, 100 mM NaCl) and 50 mM TEAB. Finally the purified membranes were solubilized in SDS-PAGE sample buffer containing 20% SDS**.** Proteins were analysed using GeLC-MSMS analysing the resulting tryptic digests using an UPLC coupled to an LTQ-Orbitrap. In addition to the two biological replicates, a technical replicate, M2b, was performed. For this replicate, the proteins of M2a were separated and analysed with GeLC-MSMS for a second time. The data-analysis and relative quantification of the proteins was performed as described in Supporting Information (Table S1).

Determination of the localization of PrsA

Single colonies of *B. subtilis* 168 and IH8478 (*prsA-myc*) grown on TY plates were used to inoculate 5 ml of TY liquid medium. Overnight cultures were diluted in 20 ml of TY medium to $OD_{600} = 0.1$ and grown till stationary phase. TY medium was supplemented with erythromycin to a final concentration of 1 μg ml^{-1} when needed. Samples for immunofluorescence assay were collected 2 h before and 4 h after the transition from the exponential to the stationary growth phase (Fig. 6). Immunofluorescence staining was performed according to the method described by Harry and collaborators (Harry *et al.*, 1995) with the modifications described below.

Cells were fixed and made permeable as follows. 0.5 ml of bacterial culture in TY was mixed with an equal volume of 2×fixative solution containing 2.68% paraformaldehyde and 0.0050% glutaraldehyde and incubated for 15 min at room temperature (21–23°C) and 30 min on ice. After fixation the cells were washed three times in PBS and resuspended in GTE (50 mM glucose, 20 mM Tris-HCl pH 7.5, 10 mM EDTA). A fresh lysozyme solution in GTE was added to an aliquot of cells to a final concentration of 2 mg ml^{-1} and cells were immediately spotted on multiwell slides (MP Biomedicals LLC) coated with 0.01% poly-L-lysine (Sigma-Aldrich). After 5 min incubation wells were washed with PBS and left to air dry.

For immunostaining, cells were blocked with PBS containing 2% BSA and 0.01% Tween (hereafter referred to as 'blocking solution') for 15 min at room temperature. Next cells were incubated with mouse anti-c-Myc antibodies (Gentaur) diluted 1:1000 in the blocking solution for 1 h at room temperature. After washing the cells 10 times with PBS, secondary anti-mouse biotin-conjugated antibody (Sigma-Aldrich) diluted 1:500 in the blocking solution was added, followed by incubation in the dark at room temperature for 1 h. Cells were washed again 10 times with PBS and incubated 1 h with 1:25 diluted ExtrAvidin Cy3 conjugate (Sigma-Aldrich) at room temperature in the dark. Samples were washed 10 times with PBS and mounted with Vectashield mounting medium (Vector Laboratories). Slides were stored at –20°C.

Sample imaging was performed using a wide-field Zeiss Axioscop50 fluorescence microscope (Carl Zeiss, Oberkochen, Germany) equipped with a Princeton Instruments 1300Y digital camera. Cy3 fluorescence was visualized with a bandpass (546 /12 nm) excitation filter, a 560 nm dichromatic mirror, and a bandpass (575–640 nm) emission filter. Images were analysed using ImageJ (http://rsb.info.nih.gov/nih-image/) and Adobe Photoshop CS2. Wide-field images were corrected for bleaching and unstable illumination using the Huygens Professional deconvolution software by Scientific Volume Imaging (http://www.svi.nl/).

Cross-linking of PrsA

Protein cross-linking was performed with 1% formaldehyde as has been described (Jensen *et al.*, 2005). Bacteria were grown in LB medium at 37°C until culture density was 100 Klett units. Cells were harvested from 1 ml of the culture, washed once with 1 ml 0.1 M sodium phosphate buffer (pH 6.8) and cross-linked with formaldehyde for 10 min at room temperature. Cells were pelleted, washed once in phosphate buffer and solubilized in SDS-PAGE lysis buffer as has been described (Healy *et al.*, 1991). Cross-linked PrsA or PrsA-Myc proteins were analysed by SDS-PAGE and immunoblotting. Samples were heated either at 37°C for 10 min or at 95°C for 30 min (breaks formaldehyde cross-links) prior to SDS-PAGE.

Acknowledgements

This work, as part of the European Science Foundation EUROCORES Programme EuroSCOPE, is supported by funds from the European Commission's Sixth Framework Programme under contract ERAS-CT-2003-980409. The work was also supported from the grants 107438, 113846 and 123318 from the Academy of Finland. BCM was supported by a grant from ALW-NWO in the Bacell SysMO programma.

We would like to thank the Department of Molecular Cell Biology of the University of Groningen, the Netherlands, for giving access to microscopy facilities and A. M. Krikken for fluorescence microscopy support. We want to thank David Popham (Virginia Tech) and Mark Leaver (Newcastle University) for several PBP mutants and gene constructs. We are also grateful to Sanna Marjavaara (University of Helsinki) for assistance in image acquisition and quantification of Bocillin-FL-labelled samples.

References

Alonzo, F. 3rd, Port, G.C., Cao, M., and Freitag, N.E. (2009) The posttranslocation chaperone PrsA2 contributes to multiple facets of *Listeria monocytogenes* pathogenesis. *Infect Immun* **77:** 2612–2623.

Antelmann, H., Darmon, E., Noone, D., Veening, J.W., Westers, H., Bron, S., *et al.* (2003) The extracellular proteome of *Bacillus subtilis* under secretion stress conditions. *Mol Microbiol* **49:** 143–156.

Atrih, A., Bacher, G., Allmaier, G., Williamson, M.P., and Foster, S.J. (1999) Analysis of peptidoglycan structure from vegetative cells of *Bacillus subtilis* 168 and role of PBP 5 in peptidoglycan maturation. *J Bacteriol* **181:** 3956–3966.

Behrens, S., Maier, R., de Cock, H., Schmid, F.X., and Gross, C.A. (2001) The SurA periplasmic PPIase lacking its parvulin domains functions in vivo and has chaperone activity. *EMBO J* **20:** 285–294.

Bramkamp, M., Weston, L., Daniel, R.A., and Errington, J. (2006) Regulated intramembrane proteolysis of FtsL protein and the control of cell division in *Bacillus subtilis*. *Mol Microbiol* **62:** 580–591.

Carballido-Lopez, R., and Errington, J. (2003) The bacterial cytoskeleton: *in vivo* dynamics of the actin-like protein Mbl of *Bacillus subtilis*. *Dev Cell* **4:** 19–28.

Carballido-Lopez, R., Formstone, A., Li, Y., Ehrlich, S.D., Noirot, P., and Errington, J. (2006) Actin homolog MreBH governs cell morphogenesis by localization of the cell wall hydrolase LytE. *Dev Cell* **11:** 399–409.

Claessen, D., Emmins, R., Hamoen, L.W., Daniel, R.A., Err-

ington, J., and Edwards, D.H. (2008) Control of the cell elongation-division cycle by shuttling of PBP1 protein in *Bacillus subtilis*. *Mol Microbiol* **68:** 1029–1046.
Courtin, P., Miranda, G., Guillot, A., Wessner, F., Mezange, C., Domakova, E., *et al*. (2006) Peptidoglycan structure analysis of *Lactococcus lactis* reveals the presence of an L,d-carboxypeptidase involved in peptidoglycan maturation. *J Bacteriol* **188:** 5293–5298.
Daniel, R.A., and Errington, J. (2003) Control of cell morphogenesis in bacteria: two distinct ways to make a rod-shaped cell. *Cell* **113:** 767–776.
Daniel, R.A., Harry, E.J., Katis, V.L., Wake, R.G., and Errington, J. (1998) Characterization of the essential cell division gene *ftsL*(*yIID*) of *Bacillus subtilis* and its role in the assembly of the division apparatus. *Mol Microbiol* **29:** 593–604.
Daniel, R.A., Noirot-Gros, M.F., Noirot, P., and Errington, J. (2006) Multiple interactions between the transmembrane division proteins of *Bacillus subtilis* and the role of FtsL instability in divisome assembly. *J Bacteriol* **188:** 7396–7404.
Darmon, E., Noone, D., Masson, A., Bron, S., Kuipers, O.P., Devine, K.M., and van Dijl, J.M. (2002) A novel class of heat and secretion stress-responsive genes is controlled by the autoregulated CssRS two-component system of *Bacillus subtilis*. *J Bacteriol* **184:** 5661–5671.
Defeu Soufo, H.J., and Graumann, P.L. (2004) Dynamic movement of actin-like proteins within bacterial cells. *EMBO Rep* **5:** 789–794.
Defeu Soufo, H.J., and Graumann, P.L. (2006) Dynamic localization and interaction with other *Bacillus subtilis* actin-like proteins are important for the function of MreB. *Mol Microbiol* **62:** 1340–1356.
Divakaruni, A.V., Loo, R.R., Xie, Y., Loo, J.A., and Gober, J.W. (2005) The cell-shape protein MreC interacts with extracytoplasmic proteins including cell wall assembly complexes in *Caulobacter crescentus*. *Proc Natl Acad Sci USA* **102:** 18602–18607.
Divakaruni, A.V., Baida, C., White, C.L., and Gober, J.W. (2007) The cell shape proteins MreB and MreC control cell morphogenesis by positioning cell wall synthetic complexes. *Mol Microbiol* **66:** 174–188.
Drouault, S., Anba, J., Bonneau, S., Bolotin, A., Ehrlich, S.D., and Renault, P. (2002) The peptidyl-prolyl isomerase motif is lacking in PmpA, the PrsA-like protein involved in the secretion machinery of *Lactococcus lactis*. *Appl Environ Microbiol* **68:** 3932–3942.
Ellermeier, C.D., and Losick, R. (2006) Evidence for a novel protease governing regulated intramembrane proteolysis and resistance to antimicrobial peptides in *Bacillus subtilis*. *Genes Dev* **20:** 1911–1922.
van den Ent, F., Leaver, M., Bendezu, F., Errington, J., de Boer, P., and Lowe, J. (2006) Dimeric structure of the cell shape protein MreC and its functional implications. *Mol Microbiol* **62:** 1631–1642.
Eymann, C., Dreisbach, A., Albrecht, D., Bernhardt, J., Becher, D., Gentner, S., *et al*. (2004) A comprehensive proteome map of growing *Bacillus subtilis* cells. *Proteomics* **4:** 2849–2876.
Figge, R.M., Divakaruni, A.V., and Gober, J.W. (2004) MreB, the cell shape-determining bacterial actin homologue, co-ordinates cell wall morphogenesis in *Caulobacter crescentus*. *Mol Microbiol* **51:** 1321–1332.
Formstone, A., and Errington, J. (2005) A magnesium-dependent *mreB* null mutant: implications for the role of *mreB* in *Bacillus subtilis*. *Mol Microbiol* **55:** 1646–1657.
Glauner, B. (1988) Separation and quantification of muropeptides with high-performance liquid chromatography. *Anal Biochem* **172:** 451–464.
Glauner, B., Holtje, J.V., and Schwarz, U. (1988) The composition of the murein of *Escherichia coli*. *J Biol Chem* **263:** 10088–10095.
Hani, J., Schelbert, B., Bernhardt, A., Domdey, H., Fischer, G., Wiebauer, K., and Rahfeld, J.U. (1999) Mutations in a peptidylprolyl-*cis*/*trans*-isomerase gene lead to a defect in 3′-end formation of a pre-mRNA in *Saccharomyces cerevisiae*. *J Biol Chem* **274:** 108–116.
Harry, E.J., Pogliano, K., and Losick, R. (1995) Use of immunofluorescence to visualize cell-specific gene expression during sporulation in *Bacillus subtilis*. *J Bacteriol* **177:** 3386–3393.
Healy, J., Weir, J., Smith, I., and Losick, R. (1991) Post-transcriptional control of a sporulation regulatory gene encoding transcription factor sigma H in *Bacillus subtilis*. *Mol Microbiol* **5:** 477–487.
Heikkinen, O., Seppala, R., Tossavainen, H., Heikkinen, S., Koskela, H., Permi, P., and Kilpelainen, I. (2009) Solution structure of the parvulin-type PPIase domain of *Staphylococcus aureus* PrsA – implications for the catalytic mechanism of parvulins. *BMC Struct Biol* **9:** 17.
Heinrich, J., Lunden, T., Kontinen, V.P., and Wiegert, T. (2008) The *Bacillus subtilis* ABC transporter EcsAB influences intramembrane proteolysis through RasP. *Microbiology* **154:** 1989–1997.
Hennecke, G., Nolte, J., Volkmer-Engert, R., Schneider-Mergener, J., and Behrens, S. (2005) The periplasmic chaperone SurA exploits two features characteristic of integral outer membrane proteins for selective substrate recognition. *J Biol Chem* **280:** 23540–23548.
Hyyryläinen, H.-L., Vitikainen, M., Thwaite, J., Wu, H., Sarvas, M., Harwood, C., *et al*. (2000) d-alanine substitution of teichoic acids as a modulator of protein folding and stability at the cytoplasmic membrane/cell wall interface of *Bacillus subtilis*. *J Biol Chem* **275:** 26696–26703.
Hyyryläinen, H.L., Bolhuis, A., Darmon, E., Muukkonen, L., Koski, P., Vitikainen, M., *et al*. (2001) A novel two-component regulatory system in *Bacillus subtilis* for the survival of severe secretion stress. *Mol Microbiol* **41:** 1159–1172.
Hyyrylainen, H.L., Sarvas, M., and Kontinen, V.P. (2005) Transcriptome analysis of the secretion stress response of *Bacillus subtilis*. *Appl Microbiol Biotechnol* **67:** 389–396.
Jacobs, M., Andersen, J.B., Kontinen, V., and Sarvas, M. (1993) *Bacillus subtilis* PrsA is required *in vivo* as an extracytoplasmic chaperone for secretion of active enzymes synthesized either with or without pro-sequences. *Mol Microbiol* **8:** 957–966.
Jensen, S.O., Thompson, L.S., and Harry, E.J. (2005) Cell division in *Bacillus subtilis*: FtsZ and FtsA association is Z-ring independent, and FtsA is required for efficient midcell Z-Ring assembly. *J Bacteriol* **187:** 6536–6544.
Jones, L.J., Carballido-Lopez, R., and Errington, J. (2001)

Control of cell shape in bacteria: helical, actin-like filaments in *Bacillus subtilis*. *Cell* **104:** 913–922.
Kalinowski, J., Bathe, B., Bartels, D., Bischoff, N., Bott, M., Burkovski, A., *et al*. (2003) The complete *Corynebacterium glutamicum* ATCC 13032 genome sequence and its impact on the production of L-aspartate-derived amino acids and vitamins. *J Biotechnol* **104:** 5–25.
Kaltwasser, M., Wiegert, T., and Schumann, W. (2002) Construction and application of epitope- and green fluorescent protein-tagging integration vectors for *Bacillus subtilis*. *Appl Environ Microbiol* **68:** 2624–2628.
Katis, V.L., and Wake, R.G. (1999) Membrane-bound division proteins DivIB and DivIC of *Bacillus subtilis* function solely through their external domains in both vegetative and sporulation division. *J Bacteriol* **181:** 2710–2718.
Kawai, Y., Daniel, R.A., and Errington, J. (2009) Regulation of cell wall morphogenesis in *Bacillus subtilis* by recruitment of PBP1 to the MreB helix. *Mol Microbiol* **71:** 1131–1144.
Kontinen, V., and Sarvas, M. (1993) The PrsA lipoprotein is essential for protein secretion in *Bacillus subtilis* and sets a limit for high-level secretion. *Mol Microbiol* **8:** 727–737.
Kühlewein, A., Voll, G., Hernandez Alvarez, B., Kessler, H., Fischer, G., Rahfeld, J.U., and Gemmecker, G. (2004) Solution structure of *Escherichia coli* Par10: The prototypic member of the Parvulin family of peptidyl-prolyl *cis/trans* isomerases. *Protein Sci* **13:** 2378–2387.
Kunst, F., Ogasawara, N., Moszer, I., Albertini, A.M., Alloni, G., Azevedo, V., *et al*. (1997) The complete genome sequence of the gram-positive bacterium *Bacillus subtilis*. *Nature* **390:** 249–256.
Leaver, M., and Errington, J. (2005) Roles for MreC and MreD proteins in helical growth of the cylindrical cell wall in *Bacillus subtilis*. *Mol Microbiol* **57:** 1196–1209.
Letek, M., Ordonez, E., Vaquera, J., Margolin, W., Flardh, K., Mateos, L.M., and Gil, J.A. (2008) DivIVA is required for polar growth in the MreB-lacking rod-shaped actinomycete *Corynebacterium glutamicum*. *J Bacteriol* **190:** 3283–3292.
Lindholm, A., Ellmen, U., Tolonen-Martikainen, M., and Palva, A. (2006) Heterologous protein secretion in *Lactococcus lactis* is enhanced by the *Bacillus subtilis* chaperone-like protein PrsA. *Appl Microbiol Biotechnol* **73:** 904–914.
Lu, K.P., and Zhou, X.Z. (2007) The prolyl isomerase PIN1: a pivotal new twist in phosphorylation signalling and disease. *Nat Rev Mol Cell Biol* **8:** 904–916.
Lu, K.P., Hanes, S.D., and Hunter, T. (1996) A human peptidyl-prolyl isomerase essential for regulation of mitosis. *Nature* **380:** 544–547.
Lu, P.J., Zhou, X.Z., Shen, M., and Lu, K.P. (1999) Function of WW domains as phosphoserine- or phosphothreonine-binding modules. *Science* **283:** 1325–1328.
Ma, Y., Bryant, A.E., Salmi, D.B., Hayes-Schroer, S.M., McIndoo, E., Aldape, M.J., and Stevens, D.L. (2006) Identification and characterization of bicistronic *speB* and *prsA* gene expression in the group A *Streptococcus*. *J Bacteriol* **188:** 7626–7634.
McPherson, D.C., Driks, A., and Popham, D.L. (2001) Two class A high-molecular-weight penicillin-binding proteins of *Bacillus subtilis* play redundant roles in sporulation. *J Bacteriol* **183:** 6046–6053.
Margot, P., and Karamata, D. (1996) The *wprA* gene of *Bacillus subtilis* 168, expressed during exponential growth, encodes a cell-wall-assosciated protease. *Microbiology* **142:** 3437–3444.
Pedersen, L.B., Angert, E.R., and Setlow, P. (1999) Septal localization of penicillin-binding protein 1 in *Bacillus subtilis*. *J Bacteriol* **181:** 3201–3211.
Pinho, M.G., and Errington, J. (2003) Dispersed mode of *Staphylococcus aureus* cell wall synthesis in the absence of the division machinery. *Mol Microbiol* **50:** 871–881.
Popham, D.L., and Setlow, P. (1995) Cloning, nucleotide sequence, and mutagenesis of the *Bacillus subtilis ponA* operon, which codes for penicillin-binding protein (PBP) 1 and a PBP-related factor. *J Bacteriol* **177:** 326–335.
Popham, D.L., and Setlow, P. (1996) Phenotypes of *Bacillus subtilis* mutants lacking multiple class a high-molecular-weight penicillin-binding proteins. *J Bacteriol* **178:** 2079–2085.
Popham, D.L., and Young, K.D. (2003) Role of penicillin-binding proteins in bacterial cell morphogenesis. *Curr Opin Microbiol* **6:** 594–599.
Popham, D.L., Helin, J., Costello, C.E., and Setlow, P. (1996) Analysis of the peptidoglycan structure of *Bacillus subtilis* endospores. *J Bacteriol* **178:** 6451–6458.
Rahfeld, J.-U., Rücknagel, K.P., Schelbert, B., Ludvig, B., Hacker, J., Mann, K., and Fischer, G. (1994) Confirmation of the existence of a third family among peptidyl-prolyl *cis*/*trans* isomerases. Amino acid sequence and recombinant production of parvulin. *FEBS Lett* **352:** 180–184.
Robson, S.A., and King, G.F. (2006) Domain architecture and structure of the bacterial cell division protein DivIB. *Proc Natl Acad Sci USA* **103:** 6700–6705.
Rodgers, K.K., Bu, Z., Fleming, K.G., Schatz, D.G., Engelman, D.M., and Coleman, J.E. (1996) A zinc-binding domain involved in the dimerization of RAG1. *J Mol Biol* **260:** 70–84.
Sauvage, E., Kerff, F., Terrak, M., Ayala, J.A., and Charlier, P. (2008) The penicillin-binding proteins: structure and role in peptidoglycan biosynthesis. *FEMS Microbiol Rev* **32:** 234–258.
Scheffers, D.J., Jones, L.J., and Errington, J. (2004) Several distinct localization patterns for penicillin-binding proteins in *Bacillus subtilis*. *Mol Microbiol* **51:** 749–764.
Schiene, C., and Fischer, G. (2000) Enzymes that catalyse the restructuring of proteins. *Curr Opin Struct Biol* **10:** 40–45.
Soufo, H.J., and Graumann, P.L. (2003) Actin-like proteins MreB and Mbl from *Bacillus subtilis* are required for bipolar positioning of replication origins. *Curr Biol* **13:** 1916–1920.
Spiess, C., Beil, A., and Ehrmann, M. (1999) A temperature-dependent switch from chaperone to protease in a widely conserved heat shock protein. *Cell* **97:** 339–347.
Stephenson, K., and Harwood, C.R. (1998) Influence of a cell-wall-associated protease on production of α-amylase by *Bacillus subtilis*. *Appl Environ Microbiol* **64:** 2875–2881.
Stewart, G.C. (2005) Taking shape: control of bacterial cell wall biosynthesis. *Mol Microbiol* **57:** 1177–1181.
Stulke, J., Hanschke, R., and Hecker, M. (1993) Temporal activation of beta-glucanase synthesis in *Bacillus subtilis* is mediated by the GTP pool. *J Gen Microbiol* **139:** 2041–2045.

Stymest, K.H., and Klappa, P. (2008) The periplasmic peptidyl prolyl *cis-trans* isomerases PpiD and SurA have partially overlapping substrate specificities. *FEBS J* **275:** 3470–3479.

Tiyanont, K., Doan, T., Lazarus, M.B., Fang, X., Rudner, D.Z., and Walker, S. (2006) Imaging peptidoglycan biosynthesis in *Bacillus subtilis* with fluorescent antibiotics. *Proc Natl Acad Sci USA* **103:** 11033–11038.

Uchida, T., Fujimori, F., Tradler, T., Fischer, G., and Rahfeld, J.-U. (1999) Identification and characterization of a 14 kDa human protein as a novel parvulin like peptidyl-prolyl *cis/trans* isomerase. *FEBS Lett* **446:** 278–282.

Vitikainen, M., Pummi, T., Airaksinen, U., Wu, H., Sarvas, M., and Kontinen, V.P. (2001) Quantitation of the capacity of the secretion apparatus and requirement for PrsA in growth and secretion of α-amylase in *Bacillus subtilis*. *J Bacteriol* **183:** 1881–1890.

Vitikainen, M., Lappalainen, I., Seppala, R., Antelmann, H., Boer, H., Taira, S., *et al*. (2004) Structure-function analysis of PrsA reveals roles for the parvulin-like and flanking N- and C-terminal domains in protein folding and secretion in *Bacillus subtilis*. *J Biol Chem* **279:** 19302–19314.

Vitikainen, M., Hyyrylainen, H.L., Kivimaki, A., Kontinen, V.P., and Sarvas, M. (2005) Secretion of heterologous proteins in *Bacillus subtilis* can be improved by engineering cell components affecting post-translocational protein folding and degradation. *J Appl Microbiol* **99:** 363–375.

Wahlstrom, E., Vitikainen, M., Kontinen, V.P., and Sarvas, M. (2003) The extracytoplasmic folding factor PrsA is required for protein secretion only in the presence of the cell wall in *Bacillus subtilis*. *Microbiology* **149:** 569–577.

Wang, P., and Heitman, J. (2005) The cyclophilins. *Genome Biol* **6:** 226.

Wei, Y., Havasy, T., McPherson, D.C., and Popham, D.L. (2003) Rod shape determination by the *Bacillus subtilis* class B penicillin-binding proteins encoded by *pbpA* and *pbpH*. *J Bacteriol* **185:** 4717–4726.

Williams, R.C., Rees, M.L., Jacobs, M.F., Pragai, Z., Thwaite, J.E., Baillie, L.W., *et al*. (2003) Production of *Bacillus anthracis* protective antigen is dependent on the extracellular chaperone, PrsA. *J Biol Chem* **278:** 18056–18062.

Wu, S.C., Ye, R., Wu, X.C., Ng, S.C., and Wong, S.L. (1998) Enhanced secretory production of a single-chain antibody fragment from *Bacillus subtilis* by coproduction of molecular chaperones. *J Bacteriol* **180:** 2830–2835.

Wu, X., Wilcox, C.B., Devasahayam, G., Hackett, R.L., Arevalo-Rodriguez, M., Cardenas, M.E., *et al*. (2000) The Ess1 prolyl isomerase is linked to chromatin remodeling complexes and the general transcription machinery. *EMBO J* **19:** 3727–3738.

Yaffe, M.B., Schutkowski, M., Shen, M., Zhou, X.Z., Stukenberg, P.T., Rahfeld, J.U., *et al*. (1997) Sequence-specific and phosphorylation-dependent proline isomerization: a potential mitotic regulatory mechanism. *Science* **278:** 1957–1960.

Yao, J.L., Kops, O., Lu, P.J., and Lu, K.P. (2001) Functional conservation of phosphorylation-specific prolyl isomerases in plants. *J Biol Chem* **276:** 13517–13523.

Zemansky, J., Kline, B.C., Woodward, J.J., Leber, J.H., Marquis, H., and Portnoy, D.A. (2009) Development of a mariner-based transposon and identification of *Listeria monocytogenes* determinants, including the peptidyl-prolyl isomerase PrsA2, that contribute to its hemolytic phenotype. *J Bacteriol* **191:** 3950–3964.

Zhao, G., Meier, T.I., Kahl, S.D., Gee, K.R., and Blaszczak, L.C. (1999) BOCILLIN FL, a sensitive and commercially available reagent for detection of penicillin-binding proteins. *Antimicrob Agents Chemother* **43:** 1124–1128.

Supporting information

Additional supporting information may be found in the online version of this article.

Please note: Wiley-Blackwell are not responsible for the content or functionality of any supporting materials supplied by the authors. Any queries (other than missing material) should be directed to the corresponding author for the article.